THE
PHYSICAL
SOCIETY

# MEMOIRS

OF THE

# COLLEGE OF SCIENCE

UNIVERSITY OF KYOTO

SERIES A

VOL. XXVIII, No. 3

September, 1957

KYOTO

MEMOIRS OF THE COLLEGE OF SCIENCE, University of Kyoto, Series A,
Vol. XXVIII, No. 3, Article 1, 1957

# DIFFRACTION OF ELECTROMAGNETIC WAVES BY A CIRCULAR CYLINDER OF INFINITE LENGTH*

BY

**Isao TAKAHASHI, Tadashi WATANABE and Kiichi TANIMOTO**

(*Received May 28, 1957*)

ABSTRACT

The diffraction of electromagnetic plane waves by a circular cylinder of infinite length is discussed in case when the wave is incident normally to the axis of the cylinder and the magnetic and the electric fields are parallel and perpendicular to the cylinder-axis respectively.

## 1. Introduction

The problems on the diffraction of electromagnetic waves by a circular cylinder have been treated by several authors. Recently, C. H. Papas (**1**) has calculated the total scattering cross section of a circular cylinder of infinite length for the plane wave incident normally to the cylinder-axis, in case when the electric field of the incident wave is parallel to the cylinder-axis and the magnetic field perpendicular to it. In this paper, the authors discuss a case in which the magnetic field is parallel to the cylinder-axis and the electric field perpendicular to it. While Papas calculated the cross section at high frequencies only to the zeroth approximation for his case, we shall here perform the calculation to the first approximation for our present case.

## 2. Fundamental equations

We assume that (1) a circular cylinder of radius $a$ is perfectly conducting, (2) the external medium is vacuum with constants $\varepsilon_0$ and $\mu_0$, and (3) the wave incident normally to the cylinder-axis has its $\boldsymbol{H}$-vector parallel to the axis and its $\boldsymbol{E}$-vector perpendicular to it. Taking the $z$-axis along the cylinder-axis, the fundamental equations in the cylindrical coordinates $\rho$, $\varphi$, $z$ are given by

$$\left.\begin{aligned} -i\omega\varepsilon_0 E_\rho &= \frac{1}{\rho}\frac{\partial H_z}{\partial \varphi}, \\ -i\omega\varepsilon_0 E_\varphi &= -\frac{\partial H_z}{\partial \rho}, \end{aligned}\right\} \qquad (1)$$

* Read at the annual meeting of the Physical Society of Japan, November 2, 1950. Some of the results here given are quoted from our manuscript, which was sent to Dr. Papas in 1951, in F. E. Borgnis and C. H. Papas's book entitled "*Randwertprobleme der Mikrowellenphysik*" (Springer Verlag, 1955), pp. 59–60.

$$i\omega\mu_0 H_z = \frac{1}{\rho}\frac{\partial}{\partial\rho}(\rho E_\varphi) - \frac{1}{\rho}\frac{\partial E_\rho}{\partial\varphi}\,, \tag{2}$$

where we have assumed $E_z = H_\rho = H_\varphi = 0$ since the state of polarization of the incident wave and the infinite length of the circular cylinder justify this assumption, and the time dependence of $\boldsymbol{E}$ and $\boldsymbol{H}$ is expressed by $e^{-i\omega t}$.

Writing $H_z = \psi$, $k^2 = \varepsilon_0\mu_0\omega^2$, we obtain, from (1) and (2),

$$(\Delta_2 + k^2)\psi = 0\,, \tag{3}$$

where $\Delta_2$ is the two-dimensional Laplacian.

Further, introducing two-dimensional Green's function $G$ defined by

$$(\Delta_2 + k^2)G(\rho,\ \varphi\,;\ \rho',\ \varphi') = -\frac{\delta(\rho-\rho')}{\rho}\delta(\varphi-\varphi')\,, \tag{4}$$

we have, by Green's theorem,

$$\int_v \Big\{G(\rho,\ \varphi\,;\ \rho',\ \varphi')(\Delta_2' + k^2)\psi(\rho',\ \varphi') - \psi(\rho',\ \varphi')(\Delta_2' + k^2)G(\rho,\ \varphi\,;\ \rho',\ \varphi')\Big\}dv'$$
$$= \int_{S_1+S_2}\Big\{G(\rho,\ \varphi\,;\ \rho',\ \varphi')\frac{\partial}{\partial n'}\psi(\rho',\ \varphi') - \psi(\rho',\ \varphi')\frac{\partial}{\partial n'}G(\rho,\ \varphi\,;\ \rho',\ \varphi')\Big\}dS'\,,$$

where $v$ is the volume of the hollow cylinder of unit length formed by the conducting cylinder surface $S_1$ of radius $a$ and the cylindrical surface $S_2$ of radius $a'$ ($>a$). A solution of (4) is

$$G(\rho,\ \varphi\,;\ \rho',\ \varphi') = \frac{i}{4}H_0^{(1)}(kx)\,, \tag{5}$$

with

$$x = \{\rho^2 + \rho'^2 - 2\rho\rho'\cos(\varphi-\varphi')\}^{\frac{1}{2}}\,.$$

In the limit $a'\to\infty$, by (3), (4), the second equation of (1) and the boundary condition on the conducting cylinder surface, the above relation from Green's theorem is rewritten as:

$$\psi(\rho,\ \varphi) = -\int_{S_1}\psi(\rho',\ \varphi')\frac{\partial}{\partial n'}G(\rho,\ \varphi\,;\ \rho',\ \varphi')dS'$$
$$+\lim_{a'\to\infty}\int_{S_2}\Big\{G(\rho,\ \varphi\,;\ \rho',\ \varphi')\frac{\partial}{\partial n'}\psi(\rho',\ \varphi') - \psi(\rho',\ \varphi')\frac{\partial}{\partial n'}G(\rho,\ \varphi\,;\ \rho',\ \varphi')\Big\}dS'\,. \tag{6}$$

Since the induced current on the conducting surface is proportional to $H_z$, namely to $\psi$, the first term of (6) can be anticipated to represent the scattered waves and accordingly, if so, the second term must represent the incident wave. In fact, if we assume the incident wave to be

$$\psi = e^{ik\rho\cos(\varphi-\varphi_1)}\,, \tag{7}$$

and put it for $\psi$ in the second term of (6), we can demonstrate

$$\lim_{a'\to\infty}\int_{S_2}\left\{G(\rho,\varphi;\rho',\varphi')\frac{\partial}{\partial n'}\psi(\rho',\varphi')-\psi(\rho',\varphi')\frac{\partial}{\partial n'}G(\rho,\varphi;\rho',\varphi')\right\}dS' = e^{ik\rho\cos(\varphi-\varphi_1)},$$

when we utilize the relations:

$$G(\rho,\varphi;\rho',\varphi')=\frac{i}{4}\sum_{n=0}^{\infty}\varepsilon_n J_n(k\rho)H_n^{(1)}(k\rho')\cos n(\varphi-\varphi'), \quad (\rho<\rho')$$

and

$$e^{ik\rho'\cos(\varphi'-\varphi_1)}=\sum_{n=0}^{\infty}\varepsilon_n i^n J_n(k\rho')\cos n(\varphi'-\varphi_1),$$

$$\text{with}\quad \varepsilon_n=\begin{cases}1 & (n=0)\\ 2 & (n\geqq 1)\end{cases}$$

Thus we obtain, instead of (6),

$$\psi(\rho,\varphi)=-\int_{S_1}\psi(\rho',\varphi')\frac{\partial}{\partial n'}G(\rho,\varphi;\rho',\varphi')dS'+e^{ik\rho\cos(\varphi-\varphi_1)}. \tag{8}$$

Considering that the value of $\partial\psi(\rho,\varphi)/\partial\rho$ at $\rho=a$ vanishes because of the second equation of (1) and the boundary condition, and that $\partial/\partial n'=-\partial/\partial\rho'$, the following equation can be shown to hold:

$$-ik\cos(\varphi-\varphi_1)\exp[ika\cos(\varphi-\varphi_1)]=a\int_0^{2\pi}\psi(a,\varphi')g(\varphi-\varphi')d\varphi', \tag{9}$$

where

$$g(\varphi-\varphi')=\left\{\frac{\partial^2}{\partial\rho\partial\rho'}G(\rho,\varphi;\rho',\varphi')\right\}_{\substack{\rho=a\\ \rho'=a}}. \tag{10}$$

If we can solve the integral equation (9) with respect to $\psi(a,\varphi')$ i.e. $H_z$ on the conducting surface, we can obtain, by putting $\psi(a,\varphi')$ into (8), the general $H_z$, i.e. $\psi(\rho,\varphi)$.

### 3. Scattering cross section

The scattered field term of (8) is:

$$\varphi^{\text{scat}}(\rho,\varphi)=a\int_0^{2\pi}\psi(a,\varphi')\left\{\frac{\partial}{\partial\rho'}G(\rho,\varphi;\rho',\varphi')\right\}_{\rho'=a}d\varphi'.$$

We shall find its asymptotic representation at $\rho\to\infty$. Since

$$G(\rho,\varphi;\rho',\varphi')\simeq\frac{i}{4}\left(\frac{-2i}{\pi k\rho}\right)^{\frac{1}{2}}\exp[ik\{\rho-\rho'\cos(\varphi-\varphi')\}]$$

holds at $\rho'\ll\rho\to\infty$, we obtain

$$\psi^{\text{scat}}(\rho,\varphi)=\frac{k}{4}\left(\frac{-2i}{\pi k}\right)^{\frac{1}{2}}\frac{1}{\sqrt{\rho}}\exp(ik\rho)A(\varphi,\varphi_1), \tag{11}$$

where

$$A(\varphi,\ \varphi_1)=a\int_0^{2\pi}\psi_{\varphi_1}(a,\ \varphi')\cos(\varphi-\varphi')\exp\{-ika\cos(\varphi-\varphi')\}d\varphi',\tag{12}$$

and the subscript $\varphi_1$ of $\psi_{\varphi_1}$ means that the corresponding incident wave propagates in the $\varphi_1$ direction. Then, from the geometrical symmetry with respect to two incident angles $\varphi_1$ and $\varphi_2$, there follows

$$A(\pi+\varphi_1,\ \varphi_2)=A(\pi+\varphi_2,\ \varphi_1)\,.\tag{13}$$

From (12) and the integral equation (9), we obtain

$$\frac{ik}{A(\pi+\varphi_2,\ \varphi_1)}=\frac{ik}{A(\pi+\varphi_1,\ \varphi_2)}$$
$$=\frac{\int_0^{2\pi}\int_0^{2\pi}d\varphi'\psi_{\varphi_1}(a,\ \varphi')g(\varphi-\varphi')\psi_{\varphi_2}(a,\ \varphi)d\varphi}{\int_0^{2\pi}\psi_{\varphi_2}\cos(\varphi-\varphi_1)\exp\{ika\cos(\varphi-\varphi_1)\}d\varphi\int_0^{2\pi}\cos(\varphi-\varphi_2)\exp\{ika\cos(\varphi-\varphi_2)\}\psi_{\varphi_2}d\varphi}.\tag{14}$$

From (14), (12) and (9) we can derive the stationarity condition of

$$A=A(\pi+\varphi_1,\ \varphi_2)=A(\pi+\varphi_2,\ \varphi_1)\,,$$

against the variation of $\psi_{\varphi_1}$ and $\psi_{\varphi_2}$, that is, the condition for $\delta A=0$.

We shall now concern ourselves with the total scattering cross section defined by

$$\sigma=\frac{\text{The time average scattered power per unit length of cylinder-axis}}{\text{The time average incident power through unit area}}$$
$$=\bar{P}^{\text{scat}}/\bar{S}^{\text{inc}}\,.$$

Since

$$\bar{S}^{\text{inc}}=\frac{1}{2}\mathrm{Re}(\boldsymbol{E}^{\text{inc}}\times\boldsymbol{H}^{\text{inc}*})=\frac{k}{2\omega\varepsilon_0}\,,$$

and

$$\bar{P}^{\text{scat}}=\frac{1}{2}\mathrm{Re}\int_0^{2\pi}E_\varphi^{\text{scat}}(a,\ \varphi)H_z^{\text{scat}*}(a,\ \varphi)ad\varphi\,,$$

we have

$$\sigma=-\mathrm{Re}\,A(\varphi_1,\ \varphi_1)\,.\tag{15}$$

## 4. Approximation of $\sigma$ at low frequencies

If, in (14), we put $\varphi_1=0$, $\varphi_2=\pi$ and $\psi_0(a,\ \varphi)=\psi_\pi(a,\ \varphi)=1$ to the zeroth approximation, we can obtain

$$A(\pi,\ \pi)=-\frac{4}{k}\frac{J_0'(ka)}{H_0^{(1)\prime}(ka)}\,,$$

and therefore, from (15), we have

$$\sigma=\frac{4}{k}\frac{\{J_0'(ka)\}^2}{\{J_0'(ka)\}^2+\{N_0'(ka)\}^2}\,.\tag{16}$$

Now, in order to improve the approximation, we assume

$$\psi_{\varphi_1} = \sum_{n=0}^{\infty} A_n \cos n(\varphi - \varphi_1) , \tag{17}$$

where $A_n$'s are unknown coefficients. From (17) and (14)

$$\frac{ik}{A(\pi, \pi)} = -\frac{\sum_{m=0}^{\infty} \sum_{n=0}^{\infty} A_m C_{mn} A_n}{(\sum_{n=0}^{\infty} A_n B_n)^2} , \tag{18}$$

where

$$\left.\begin{aligned} B_n &= 2(-i)^n J_n'(ka) , \\ C_{mn} &= \delta_n^m \frac{(-1)^m i\pi^2 k^2}{m} J_m'(ka) H_m^{(1)\prime}(ka) . \end{aligned}\right\} \tag{19}$$

If we give variations to $A_n$'s in (18), there follows by virtue of the stationarity of $A(\pi, \pi)$,

$$\frac{A(\pi, \pi)}{ik} \sum_{n=0}^{\infty} A_n C_{mn} = -B_m \sum_{n=0}^{\infty} A_n B_n . \tag{20}$$

Further, to calculate after the method of Schwinger (**2**), we introduce $D_m$ defined by

$$\sum_{n=0}^{\infty} C_{mn} D_n = B_m , \qquad (m = 0, 1, 2, \cdots) .$$

By multiplying (20) by $D_m$ and summing up with respect to $m$, we obtain

$$\frac{A(\pi, \pi)}{ik} \sum_m \{ (\sum_n A_n C_{mn}) D_m \} = -(\sum_m D_m B_m)(\sum_n A_n B_n) ,$$

which gives

$$\frac{A(\pi, \pi)}{ik} = -\sum_m D_m B_m = -\sum_m \frac{B_m^2}{C_{mm}} .$$

Therefore, we obtain finally

$$\sigma = \frac{4}{k} \sum_{n=0}^{\infty} \varepsilon_n \frac{\{J_n'(ka)\}^2}{\{J_n'(ka)\}^2 + \{N_n'(ka)\}^2} . \tag{21}$$

As will be shown in Appendix I, this result can also be derived from the results of Ignatowsky (**3**).

In order to compare, at low frequencies, our result with that of Papas, we denote our $\sigma$ by $\sigma_\perp$ and Papas's $\sigma$ by $\sigma_{\parallel}$. Papas has given the results that

$$\sigma_{\parallel} = \frac{4}{k} \frac{\{J_0(ka)\}^2}{\{J_0(ka)\}^2 + \{N_0(ka)\}^2} ,$$

$$\sigma_{\parallel} = \frac{4}{k} \sum_{n=0}^{\infty} \varepsilon_n \frac{\{J_n(ka)\}^2}{\{J_n(ka)\}^2 + \{N_n(ka)\}^2} ,$$

which correspond respectively to (16) and (21) in our present case. Then, if we

retain only the first term in each expansion of cylindrical functions for $ka \ll 1$, we have

$$\frac{\sigma_{\perp}}{\sigma_{\parallel}} = \left\{\frac{(ka)^2}{2\ln(ka)}\right\}^2, \tag{22}$$

and

$$\frac{\sigma_{\perp}}{\sigma_{\parallel}} \to 0 \quad \text{as} \quad ka \to 0.$$

## 5. Approximation of $\sigma$ at high frequencies

In this case, we can approximate the distribution of $\psi_{\varphi_1}(a, \varphi)$ such that

$$\psi_{\varphi_1}(a, \varphi) = \sum_{n=0}^{\infty}{}' b_n \cos n(\varphi - \varphi_1) \exp\{ika\cos(\varphi - \varphi_1)\} \quad \text{on the illuminated side,}$$
$$\psi_{\varphi_1}(a, \varphi) = 0 \quad \text{on the shadow side.}$$

To the zeroth approximation, we put

$$\psi_{\varphi_1}(a, \varphi) = \exp\{ika\cos(\varphi - \varphi_1)\} \quad \text{on the illuminated side,}$$
$$\psi_{\varphi_1}(a, \varphi) = 0 \quad \text{on the shadow side,} \tag{23}$$

that is, we assume Kirchhoff's approximation.

For the sake of convenience, we consider $\psi_{\frac{\pi}{2}}$ and $\psi_{\frac{3\pi}{2}}$ as given by

$$\left.\begin{aligned} \psi_{\frac{\pi}{2}}(a, \varphi) &= \exp(ika\sin\varphi), \quad (\pi \leqq \varphi \leqq 2\pi) \\ &= 0, \quad (0 \leqq \varphi \leqq \pi) \end{aligned}\right\} \tag{24}$$

$$\left.\begin{aligned} \psi_{\frac{3\pi}{2}}(a, \varphi) &= \exp(-ika\sin\varphi), \quad (0 \leqq \varphi \leqq \pi) \\ &= 0. \quad (\pi \leqq \varphi \leqq 2\pi) \end{aligned}\right\} \tag{25}$$

Applying these to (14), we have

$$\frac{ik}{A\left(\frac{\pi}{2}, \frac{\pi}{2}\right)} = \frac{1}{4}\int_0^{\pi} d\varphi \int_{\pi}^{2\pi} \exp\{-ika(\sin\varphi - \sin\varphi')\} g(\varphi - \varphi') d\varphi'. \tag{26}$$

If we change the integration variables from $\varphi$, $\varphi'$ to $\alpha$, $\beta$ by the relations

$$\varphi - \varphi' + 2\pi = 2\alpha, \quad \varphi + \varphi' - 2\pi = 2\beta, \tag{27}$$

(26) becomes

$$\frac{ik}{A\left(\frac{\pi}{2}, \frac{\pi}{2}\right)} = 2\int_0^{\frac{\pi}{2}} g(2\alpha)\, d\alpha \int_0^{\infty} \exp(-2ika\sin\alpha\sin\beta) d\beta. \tag{28}$$

Carrying out the integration with respect to $\beta$ for $ka \gg 1$ by the method of stationary phase, we have

$$\frac{ik}{A\left(\frac{\pi}{2}, \frac{\pi}{2}\right)} = \left(\frac{i\pi}{ka}\right)^{\frac{1}{2}} \int_0^{\frac{\pi}{2}} g(2\alpha) \frac{\exp(-2ika\sin\alpha)}{\sqrt{\sin\alpha}} d\alpha, \tag{29}$$

where

$$g(2\alpha)=\frac{-ik^2}{4}\left\{H_1^{(1)'}(2ka\sin\alpha)\sin^2\alpha-\frac{1}{ka}H_1^{(1)}(2ka\sin\alpha)\frac{\cos^2\alpha}{2\sin\alpha}\right\}. \tag{30}$$

Now, $\alpha=0$ is a singular point of the integrand of (29). If $2ka\sin\alpha\gg1$, however, it can be proved that the second term of $g(2\alpha)$ gives only imaginary contribution to $A$ and thus no contribution to $\sigma$.

In order to secure the convergency of the integral, we replace the lower limit 0 by $\alpha_0$ such that $2ka\sin\alpha_0\gg1$. In this case, we write $A_{\alpha_0}(\pi/2,\ \pi/2)$ in place of $A(\pi/2,\ \pi/2)$ and (29) becomes

$$\frac{ik}{A_{\alpha_0}\left(\frac{\pi}{2},\ \frac{\pi}{2}\right)}=\frac{-ik}{4a}\int_{\alpha_0}^{\frac{\pi}{2}}\sin\alpha d\alpha=-\frac{ik}{4a}\cos\alpha_0, \tag{31}$$

when the second term of the integrand is conveniently neglected. Thus the corresponding cross section is

$$\sigma_{\alpha_0}=\frac{4a}{\cos\alpha_0}. \tag{32}$$

The dependence of $\sigma_{\alpha_0}$ on $ka$ is roughly considered as follows. For example, if we put $2ka\sin\alpha_0=10$, Hankel's function can be asymptotically expanded to a good approximation. Then, we have

$$\sigma_{\alpha_0}=\frac{4a}{\left\{1-\left(\frac{5}{ka}\right)^2\right\}^{1/2}}\approx4a\left\{1+\frac{1}{2}\left(\frac{5}{ka}\right)^2\right\}, \tag{33}$$

which enables us to anticipate the high frequency behaviour of $\sigma$. Especially it gives

$$\lim_{ka\to\infty}\sigma_{\alpha_0}=4a,$$

which coincides with the cross section in the geometrical optics.

For a better approximation of $\sigma$ calculation, we take, instead of (23), the first two terms in the expansion of $\psi_{\varphi_1}$ and thus we put

$$\begin{aligned}\psi_{\varphi_1}&=\{1+b\cos(\varphi-\varphi_1)\}\exp\{ika\cos(\varphi-\varphi_1)\} && \text{on the illuminated side,}\\ &=0 && \text{on the shadow side.}\end{aligned} \tag{34}$$

Then,

$$\begin{aligned}\psi_{\frac{\pi}{2}}&=(1+b\sin\varphi)\exp(ika\sin\varphi), && (\pi\leqq\varphi\leqq2\pi)\\ &=0, && (0\leqq\varphi\leqq\pi)\\ \psi_{\frac{3\pi}{2}}&=(1-b\sin\varphi)\exp(-ika\sin\varphi), && (0\leqq\varphi\leqq\pi)\\ &=0, && (\pi\leqq\varphi\leqq2\pi)\end{aligned}$$

which correspond respectively to (24) and (25). If we introduce these into (14), we obtain

$$\frac{ik}{A\left(\frac{\pi}{2}, \frac{\pi}{2}\right)} = \frac{P+2bQ+b^2R}{P'+2bQ'+b^2R'}, \tag{35}$$

where

$$\left.\begin{aligned}
P &= \int_{\pi}^{2\pi} \exp(ika\sin\varphi')d\varphi' \int_0^{\pi} g(\varphi-\varphi')\exp(-ika\sin\varphi)d\varphi, \\
Q &= \frac{1}{2}\int_{\pi}^{2\pi} \sin\varphi' \exp(ika\sin\varphi')d\varphi' \int_0^{\pi} g(\varphi-\varphi')\exp(-ika\sin\varphi)d\varphi \\
&\quad -\frac{1}{2}\int_{\pi}^{2\pi} \exp(ika\sin\varphi')d\varphi' \int_0^{\pi} g(\varphi-\varphi')\sin\varphi\exp(-ika\sin\varphi)d\varphi, \\
R &= -\int_{\pi}^{2\pi} \sin\varphi' \exp(ika\sin\varphi')d\varphi' \int_0^{\pi} g(\varphi-\varphi')\sin\varphi\exp(-ika\sin\varphi)d\varphi, \\
P' &= -\int_0^{\pi} \sin\varphi d\varphi \int_{\pi}^{2\pi} \sin\varphi d\varphi, \\
Q' &= \frac{1}{2}\int_0^{\pi} \sin^2\varphi d\varphi \int_{\pi}^{2\pi} \sin\varphi d\varphi - \frac{1}{2}\int_0^{\pi} \sin\varphi d\varphi \int_{\pi}^{2\pi} \sin^2\varphi d\varphi, \\
R' &= \int_0^{\pi} \sin^2\varphi d\varphi \int_{\pi}^{2\pi} \sin^2\varphi d\varphi.
\end{aligned}\right\} \tag{36}$$

Further, (35) can be transformed into

$$\frac{ik}{A\left(\frac{\pi}{2}, \frac{\pi}{2}\right)} = \frac{b_0^2P+2b_0b_1Q+b_1^2R}{b_0^2P'+2b_0b_1Q'+b_1^2R'} = \frac{\sum_{m=0}^{1}\sum_{n=0}^{1} b_m M_{mn} b_n}{\sum_{m=0}^{1}\sum_{n=0}^{1} b_m N_{mn} b_n}, \tag{37}$$

where

$$\left.\begin{aligned}
&b_0 = 1, && M_{00} = P, && N_{00} = P', \\
&b_1 = b, && M_{01} = M_{10} = Q, && N_{01} = N_{10} = Q', \\
& && M_{11} = R, && N_{11} = R'.
\end{aligned}\right\} \tag{38}$$

When we give variation to $b_m$ in (37) corresponding to the variation of $\psi_{\varphi_1}$, we have from the stationarity of $A$,

$$A\left(\frac{\pi}{2}, \frac{\pi}{2}\right)\sum_{n=0}^{1} M_{mn}b_n = ik\sum_{n=0}^{1} N_{mn}b_n. \tag{39}$$

Then, multiplying (39) with an indeterminate quantity $E_m$ and summing up with respect to $m$, we obtain

$$A\left(\frac{\pi}{2}, \frac{\pi}{2}\right) = ik\frac{\sum_m\sum_n E_m N_{mn} b_n}{\sum_m\sum_n E_m M_{mn} b_n}. \tag{40}$$

The above $E_m$ can be defined by

$$\sum_{m=0}^{1} E_m N_{mn} = \lambda \sum_{m=0}^{1} E_m M_{mn} \quad (n = 0, 1), \tag{41}$$

that is,

$$\left.\begin{aligned}(N_{00}-\lambda M_{00})E_0+(N_{10}-\lambda M_{10})E_1=0\,,\\(N_{01}-\lambda M_{01})E_0+(N_{11}-\lambda M_{11})E_1=0\,,\end{aligned}\right\} \tag{41'}$$

where $\lambda$ is an undetermined constant.

In order that a nontrivial solution of $E_m$ may exist, the following equation must be satisfied:

$$\begin{vmatrix} N_{00}-\lambda M_{00} & N_{10}-\lambda M_{10} \\ N_{01}-\lambda M_{01} & N_{11}-\lambda M_{11} \end{vmatrix} = 0\,,$$

that is,

$$\begin{vmatrix} P'-\lambda P & Q'-\lambda Q \\ Q'-\lambda Q & R'-\lambda R \end{vmatrix} = 0\,, \tag{42}$$

which determines the value of $\lambda$. Accordingly, $E_m$ $(m=0, 1)$ can also be determined, but for the determination of $A$ which in turn gives $\sigma$ by (15), it suffices only to know the value of $\lambda$, because from (40) and (41), we have

$$A\left(\frac{\pi}{2}, \frac{\pi}{2}\right) = ik\lambda\,. \tag{43}$$

For $ka \gg 1$ and $2ka\sin\alpha_0 \gg 1$, the elements of the determinantal equation (42) become:

$$\left.\begin{aligned} P &= \frac{-ik}{a}\cos\alpha_0\,,\\ Q &= \frac{ik}{2a}\left(\frac{\pi}{2}-\alpha_0+\frac{\sin 2\alpha_0}{2}\right),\\ R &= -\frac{ik}{a}\left(\cos\alpha_0-\frac{\cos^3\alpha_0}{3}\right),\\ P' &= 4\,,\\ Q' &= -\pi\,,\\ R' &= \frac{\pi^2}{4}\,, \end{aligned}\right\} \tag{36'}$$

whose derivation is shown in Appendix II. With these values, the solution of (42) is given by

$$\lambda = -\frac{a}{ik}\,\frac{4\left(\cos\alpha_0-\frac{1}{3}\cos^3\alpha_0\right)+\frac{\pi^2}{4}\cos\alpha_0-\frac{\pi^2}{2}+\pi\alpha_0-\frac{\pi}{2}\sin 2\alpha_0}{\cos\alpha_0\left(\cos\alpha_0-\frac{1}{3}\cos^3\alpha_0\right)-\frac{1}{4}\left(\frac{\pi}{2}-\alpha_0+\frac{1}{2}\sin 2\alpha_0\right)^2}\,. \tag{44}$$

To get a rough estimation, we put for example

$$2ka\sin\alpha_0 = 10\,,$$

then (44) becomes

$$\lambda = -\frac{4a}{ik}\left\{1+\frac{1}{2}\left(\frac{5}{ka}\right)^2\right\}, \tag{45}$$

and we obtain by (15)

$$\sigma = 4a\left\{1+\frac{1}{2}\left(\frac{5}{ka}\right)^2\right\}, \tag{46}$$

which tends to

$$\sigma = 4a \qquad \text{as} \quad ka \to \infty . \tag{47}$$

**Acknowledgement**

The authors' thanks are due to Professor S. Tomotika for his helpful discussion. Especially the junior author (T. W.) wishes to thank Professor Tomotika for his powerful guidance, in mathematical physics, since the time when he was an undergraduate student under the direction of Professor Tomotika.

## Appendix I

Using the results derived by Ignatowsky (**3**), $\sigma$ can be evaluated as follows. Corresponding to

$$H_z^{\text{inc}} = e^{ik\rho\cos(\varphi-\varphi_1)} = \sum_{n=0}^{\infty} \varepsilon_n i^n J_n(k\rho)\cos n(\varphi-\varphi_1), \tag{A1}$$

we put

$$H_z^{\text{scat}} = \sum_{n=0}^{\infty} \varepsilon_n i^n P_n H_n^{(1)}(k\rho)\cos n(\varphi-\varphi_1), \tag{A2}$$

where $\varepsilon_0=1$, $\varepsilon_n=2$ $(n\geqq 1)$, and $P_n$ is an unknown factor, but it can be determined by the boundary condition to be

$$P_n = -\frac{J_n'(ka)}{H_n^{(1)\prime}(ka)}. \tag{A3}$$

Inserting (A3) into (A2), we obtain

$$\begin{aligned}\sigma &= -\frac{1}{k}\operatorname{Im}\left\{\int_0^{2\pi}\left(\frac{\partial H_z^{\text{inc}}}{\partial\rho}\right)_{\rho=a} H_z^*(a,\varphi)\,a\,d\varphi\right\} \\ &= \frac{4}{k}\sum_{n=0}^{\infty}\varepsilon_n \frac{\{J_n'(ka)\}^2}{\{J_n'(ka)\}^2+\{N_n'(ka)\}^2},\end{aligned} \tag{A4}$$

which coincides with (21).

## Appendix II

The evaluation of $P'$, $Q'$ and $R'$ is easy and $P$ is equal to the right-hand side of (26) except for a numerical factor. Therefore, we perform the evaluation of $Q$ and $R$ only. Now,

$$Q = Q_1 + Q_2,$$

with

$$Q_1 = \frac{1}{2}\int_{\pi}^{2\pi} \sin\varphi' \exp(ika\sin\varphi')\,d\varphi' \int_0^{\pi} g(\varphi-\varphi')\exp(-ika\sin\varphi)\,d\varphi,$$

$$Q_2 = -\frac{1}{2}\int_{\pi}^{2\pi} \exp(ika\sin\varphi')d\varphi' \int_0^{\pi} g(\varphi-\varphi')\sin\varphi \exp(-ika\sin\varphi)d\varphi .$$

Changing the integration variables from $\varphi$, $\varphi'$ to $\alpha$, $\beta$ by the relations:

$$\varphi - \varphi' - 2\pi = 2\alpha , \quad \varphi + \varphi' - 2\pi = 2\beta ,$$

we have

$$Q_1 = -4\int_0^{\frac{\pi}{2}} d\alpha\, g(2\alpha) \int_0^{\alpha} d\beta \sin(\alpha-\beta) \exp(-2ika\sin\alpha\cos\beta) .$$

Carrying out the integration with respect to $\beta$ for $ka \gg 1$, we obtain

$$Q_1 = -2\left(\frac{i\pi}{ka}\right)^{\frac{1}{2}} \int_0^{\frac{\pi}{2}} d\alpha\, g(2\alpha)(\sin\alpha)^{\frac{1}{2}} \exp(-2ika\sin\alpha) .$$

If we replace the lower limit of the above integral by the constant $\alpha_0$ which statisfies $2ka\sin\alpha_0 \gg 1$, then

$$Q_1 = \frac{ik}{4a}\left(\frac{\pi}{2} - \alpha_0 + \frac{1}{2}\sin 2\alpha_0\right) .$$

Further, we can easily show that $Q_2 = Q_1$ and thus we obtain finally the following expression for $Q$:

$$Q = \frac{ik}{2a}\left(\frac{\pi}{2} - \alpha_0 + \frac{1}{2}\sin 2\alpha_0\right) .$$

Similarly we can evaluate $R$.

## REFERENCES


1. C. H. PAPAS, Diffraction by a cylindrical obstacle. J. Appl. Phys. **21** (1950), 314.
2. H. LEVINE and J. SCHWINGER, On the theory of diffraction by an aperture in an infinite plane screen, I. Phys. Rev. **74** (1943), 953.
3. W. v. IGNATOWSKY, Reflexion elektromagnetischer Wellen an einem Draht. Ann. d. Phys. **18** (1905), 495.

MEMOIRS OF THE COLLEGE OF SCIENCE, University of Kyoto, Series A,
Vol. XXVIII, No. 3, Article 2, 1957

# TRANSIENT PHENOMENA IN THE WAVE GUIDE*

BY

**I. TAKAHASHI and T. WATANABE**

(*Received May 28, 1957*)

ABSTRACT

Transient phenomena in the wave guide are discussed in the present paper. To this end, we deal with the case in which various modes of electromagnetic waves are excited in the wave guide by an electric or a magnetic dipole lying along the guide axis, assuming that for $t<0$, neither an electric nor a magnetic dipole exists and at $t=0$, either an electric or a magnetic dipole appears, giving rise to the excitation of the electromagnetic waves in the guide.

## 1. Introduction

With the development of microwave technique, the wave guide, one of the main components, has been discussed more in detail. The discussions, however, seem to have been confined so far to the steady-state problems, without being extended to the transient phenomena. In this paper, the authors try to treat the transient phenomena. We consider the case in which various modes of electromagnetic waves are excited in the wave guide by an electric or a magnetic dipole oriented along the guide axis on the following assumptions: For $t<0$, neither an electric nor a magnetic dipole exists, and so no field quantities exist. At $t=0$, either an electric or a magnetic dipole appears and so the electromagnetic waves are excited in the guide. On these assumptions, we derive the Hertzian vectors of excited waves.

The electric and magnetic fields can be derived by differentiating the Hertzian vectors with respect to the time and spatial coordinates.

## 2. Laplace transforms of the Maxwell equations

The Maxwell equations in the isotropic homogeneous non-dispersive medium are expressed in M. K. S. units as follows:

$$\begin{aligned} \nabla\times\boldsymbol{E}(\vec{r},\ t)+\mu\frac{\partial\boldsymbol{H}(\vec{r},\ t)}{\partial t}&=0\,,\\ \nabla\times\boldsymbol{H}(\vec{r},\ t)-\varepsilon\frac{\partial\boldsymbol{E}(\vec{r},\ t)}{\partial t}&=\boldsymbol{J}(\vec{r},\ t)\,, \end{aligned} \tag{2.1}$$

* Read at the annual meeting of the Physical Society of Japan, October 9, 1951.

$$\nabla\cdot\varepsilon\boldsymbol{E}(\vec{r},\ t)=\rho(\vec{r},\ t)\,,$$
$$\nabla\cdot\mu\boldsymbol{H}(\vec{r},\ t)=0\,.$$

Multiplying each of these equations by $e^{-pt}$ and integrating from 0 to $\infty$ with respect to $t$, namely, by operating Laplace transform, we obtain, by using the assumptions made in § 1:

$$\begin{aligned}
&\nabla\times\boldsymbol{E}(\vec{r},\ p)+\mu p\boldsymbol{H}(\vec{r},\ p)=0\,,\\
&\nabla\times\boldsymbol{H}(\vec{r},\ p)-\varepsilon p\boldsymbol{E}(\vec{r},\ p)=\boldsymbol{J}(\vec{r},\ p)\,,\\
&\nabla\cdot\varepsilon\boldsymbol{E}(\vec{r},\ p)=\rho(\vec{r},\ p)\,,\\
&\nabla\cdot\mu\boldsymbol{H}(\vec{r},\ p)=0\,,
\end{aligned}\tag{2.2}$$

where $\boldsymbol{E}(\vec{r},\ p)$, $\boldsymbol{H}(\vec{r},\ p)$, $\boldsymbol{J}(\vec{r},\ p)$ and $\rho(\vec{r},\ p)$ are Laplace transforms of $\boldsymbol{E}(\vec{r},\ t)$, $\boldsymbol{H}(\vec{r},\ t)$, $\boldsymbol{J}(\vec{r},\ t)$ and $\rho(\vec{r},\ t)$ and similar symbols will be used in the following.

When Eqs. (2.1) represent harmonic waves, that is, when the time dependence is expressed by $e^{i\omega t}$, the forms of (2.2) coincide with those which (2.1) will take, when $i\omega$ is replaced by $p$ and the time factor $e^{pt}$ is omitted. Hence, in order to solve Eqs. (2.2), it is sufficient to replace $i\omega$ in the steady-state solution by $p$.

Now, as we wish to consider the electromagnetic fields in the wave guide, the field quantities $\boldsymbol{E}(\vec{r},\ t)$, $\boldsymbol{H}(\vec{r},\ t)$ are derived from the combination of the $z$-components of the electric Hertzian vector and the magnetic Hertzian vector: $\Phi(\vec{r},\ t)$ and $\Psi(\vec{r},\ t)$. They are:

$$\begin{aligned}
E_x(\vec{r},\ t)&=\frac{\partial^2\Phi(\vec{r},\ t)}{\partial x\partial z}-\mu\frac{\partial^2\Psi(\vec{r},\ t)}{\partial t\partial y}\,,\\
E_y(\vec{r},\ t)&=\frac{\partial^2\Phi(\vec{r},\ t)}{\partial y\partial z}+\mu\frac{\partial^2\Psi(r,\ t)}{\partial t\partial x}\,,\\
E_z(\vec{r},\ t)&=\frac{\partial^2\Phi(\vec{r},\ t)}{\partial z^2}-\varepsilon\mu\frac{\partial^2\Phi(\vec{r},\ t)}{\partial t^2}\,,\\
H_x(\vec{r},\ t)&=\frac{\partial^2\Psi(\vec{r},\ t)}{\partial x\partial z}+\varepsilon\frac{\partial^2\Phi(\vec{r},\ t)}{\partial t\partial y}\,,\\
H_y(\vec{r},\ t)&=\frac{\partial^2\Psi(\vec{r},\ t)}{\partial y\partial z}-\varepsilon\frac{\partial^2\Phi(\vec{r},\ t)}{\partial t\partial x}\,,\\
H_z(\vec{r},\ t)&=\frac{\partial^2\Psi(\vec{r},\ t)}{\partial z^2}-\varepsilon\mu\frac{\partial^2\Psi(\vec{r},\ t)}{\partial t^2}\,.
\end{aligned}\tag{2.3}$$

If we take their Laplace transforms, we obtain, using the assumptions in § 1,

$$\begin{aligned}
E_x(\vec{r},\ p)&=\frac{\partial^2\Phi(\vec{r},\ p)}{\partial x\partial z}-p\mu\frac{\partial\Psi(\vec{r},\ p)}{\partial y}\,,\\
E_y(\vec{r},\ p)&=\frac{\partial^2\Phi(\vec{r},\ p)}{\partial y\partial z}+p\mu\frac{\partial\Psi(\vec{r},\ p)}{\partial x}\,,\\
E_z(\vec{r},\ p)&=\frac{\partial^2\Phi(\vec{r},\ p)}{\partial z^2}-p^2\varepsilon\mu\Phi(\vec{r},\ p)\,,
\end{aligned}\tag{2.4}$$

$$H_x(\vec{r}, p) = \frac{\partial^2 \Psi(\vec{r}, p)}{\partial x \partial z} + p\varepsilon \frac{\partial \Phi(\vec{r}, p)}{\partial y},$$

$$H_y(\vec{r}, p) = \frac{\partial^2 \Psi(\vec{r}, p)}{\partial y \partial z} - p\varepsilon \frac{\partial \Phi(\vec{r}, p)}{\partial x},$$

$$H_z(\vec{r}, p) = \frac{\partial^2 \Psi(\vec{r}, p)}{\partial z^2} - p^2 \varepsilon \mu \Psi(\vec{r}, p),$$

and also

$$\left(\Delta - \varepsilon\mu \frac{\partial^2}{\partial t^2}\right) \begin{Bmatrix} \Psi(\vec{r}, t) \\ \Phi(\vec{r}, t) \end{Bmatrix} = \begin{cases} -\dfrac{1}{\mu} M_z(t) \delta(\vec{r} - \vec{r}_0) \\ -\dfrac{1}{\varepsilon} P_z(t) \delta(\vec{r} - \vec{r}_0), \end{cases} \tag{2.5}$$

where $P_z$ and $M_z$ are respectively the $z$-components of the electric and magnetic diople moments of the exciting system located at $\vec{r} = \vec{r}_0$.

Taking the Laplace transforms of (2.5) and using the assumptions in § 1, we derive

$$(\Delta - \varepsilon\mu p^2) \begin{Bmatrix} \Psi(\vec{r}, p) \\ \Phi(\vec{r}, p) \end{Bmatrix} = \begin{cases} -\dfrac{1}{\mu} M_z(p) \delta(\vec{r} - \vec{r}_0) \\ -\dfrac{1}{\varepsilon} P_z(p) \delta(\vec{r} - \vec{r}_0). \end{cases} \tag{2.6}$$

According to (2.4) and (2.6), the Laplace transforms of electromagnetic fields in the guide are identified with the steady-state solutions in which $i\omega$ is replaced by $p$ and the time dependent factor $e^{pt}$ is omitted. This is statement made at the beginning of this section.

### 3. Laplace transforms of Hertzian vectors in the wave guide

As is well known, the electromagnetic waves in the guide that are excited by an electric or a magnetic dipole oriented in an arbitrary direction, can be expressed by a linear combination of $z$-components of electric and magnetic Hertzian vectors $\Phi(\vec{r}, t)$ and $\Psi(\vec{r}, t)$, where the $z$-axis is the guide axis. But we consider only the case in which an electric or a magnetic dipole is oriented along the $z$-axis. Other cases can be treated in the same manner. The symbols to be used in the following are summarized below.

$I(t)$ : strength of electric current forming an electric or a magnetic dipole, where the latter is considered as the elementary circulating current,

$I(p)$ : Laplace transform of $I(t)$,

$\delta\zeta$ : length of an electric dipole,

$\delta F$ : area of the elementary circulating current,

$\vec{r}_0(x_0, y_0, 0)$ : position of dipole,

$\psi_n(x, y)$ : a function defined by $\left(\frac{\partial^2}{\partial x^2}+\frac{\partial^2}{\partial y^2}+k_n^2\right)\psi_n(x, y)=0$ subject to the boundary condition $\partial\psi_n/\partial n=0$ at the wall of the wave guide, where $k_n^2$ is the $n$th eigenvalue of $\psi_n(x, y)$ and $k_n^2 \leqq k_{n+1}^2$,

$\varphi_n(x, y)$ : a function defined by $\left(\frac{\partial^2}{\partial x^2}+\frac{\partial^2}{\partial y^2}+k_n'^2\right)\varphi_n(x, y)=0$ subject to the boundary condition $\varphi_n(x, y)=0$ at the wall, where $k_n'^2$ is the $n$th eigenvalue of $\varphi_n(x, y)$ and $k_n'^2 \leqq k_{n+1}'^2$,

$$\gamma_n = (k_n^2+p^2\varepsilon\mu)^{1/2} \qquad \left(0 \leqq \arg\gamma_n \leqq \frac{\pi}{2}\right),$$

$$\gamma_n' = (k_n'^2+p^2\varepsilon\mu)^{1/2} \qquad \left(0 \leqq \arg\gamma_n' \leqq \frac{\pi}{2}\right),$$

$$J(\psi_n) = \iint \psi_n^2(x, y)dxdy,$$
$$J(\varphi_n) = \iint \varphi_n^2(x, y)dxdy.$$

According to the statement made at the beginning of § 2, the Laplace transform of an electric or a magnetic dipole moment can be expressed as follows:

The Laplace transform of a magnetic dipole moment is $\mu I(p)\delta F$ and that of an electric dipole moment $I(p)\delta\zeta/p$. Now, when an electric or a magnetic dipole is oriented along the $z$-axis, we have the following expressions which are obtained by putting $p$ in place of $i\omega$ in the usual steady-state solutions (**1**):

(i) For a magnetic dipole parallel to the $z$-axis,

$$\Psi^{mz}(\vec{r}, p) = \frac{I(p)\delta F}{2}\sum_n \frac{\psi_n(x_0, y_0)\psi_n(x, y)}{\gamma_n J(\psi_n)} e^{\mp\gamma_n z}. \tag{3.1}$$

The electromagnetic field can be derived from the Laplace transform of the $z$-component of this magnetic Hertzian vector.

(ii) For an electric dipole parallel to the $z$-axis,

$$\Phi^{ez}(\vec{r}, p) = \frac{I(p)\delta\zeta}{2\varepsilon}\sum_n \frac{\varphi_n(x_0, y_0)\varphi_n(x, y)}{p\gamma_n' J(\varphi_n)} e^{\mp\gamma_n' z}. \tag{3.2}$$

The double signs in the above two expressions are to be taken in the same order. The minus sign in the exponential factor corresponds to the waves travelling in the direction of $z$ increasing, while the plus sign corresponds to the waves travelling in the direction of $z$ decreasing, when $p$ is replaced by $i\omega$. In the following, we consider only the case in which the exponential factors are $\exp(-\gamma_n z)$ and $\exp(-\gamma_n' z)$, $(z>0)$. The case in which the

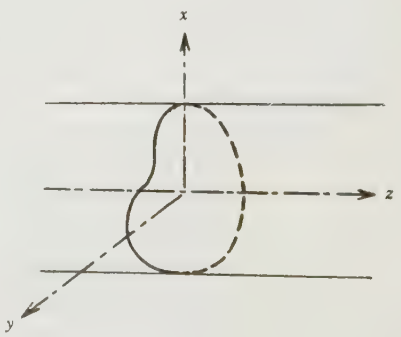


Fig. 1.

exponential factors are $\exp\begin{Bmatrix}\gamma_n z\\ \gamma'_n z\end{Bmatrix}$ $(z<0)$ can be treated analogously. Operating inverse transform to these expressions, we can obtain the corresponding $\Psi(\vec{r}, t)$ and $\Phi(\vec{r}, t)$.

**4. Case 1 when the impressed current $I_0 e^{i\omega t}$ begins to be impressed at $t=0$.**

In this case, we take

$$I(t) = \begin{cases} 0 & \text{when } t<0\,, \\ I_0 e^{i\omega t} & \text{when } t\geqq 0\,, \end{cases} \tag{4.1}$$

where $I_0$ represents a complex amplitude of current. By taking the Laplace transform of (4.1), we obtain

$$I(p) = \frac{I_0}{p-i\omega}\,.$$

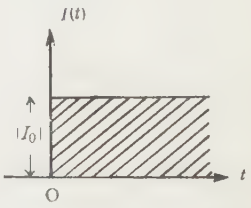

Fig. 2.

Substituting this into (3.1) and (3.2) and taking their inverse transforms, we obtain $\Psi(\vec{r}, t)$ and $\Phi(\vec{r}, t)$ for the present case.

In the case (ii) in § 3 we have (**2**), for $z>0$,

$$\begin{aligned} \frac{e^{-\gamma_n z}}{\gamma_n} &= \frac{e^{-z(k_n^2+p^2\varepsilon\mu)^{1/2}}}{(k_n^2+p^2\varepsilon\mu)^{1/2}} = \int_0^\infty J_0(k_n\beta)\frac{\exp(-p\sqrt{\varepsilon\mu}\sqrt{\beta^2+z^2})}{(\beta^2+z^2)^{1/2}}\beta d\beta \\ &= a\int_{z/a}^\infty J_0(k_n\sqrt{a^2\tau^2-z^2})e^{-p\tau}d\tau \\ &= a\phi_n(z,p)\,, \end{aligned} \tag{4.3}$$

where we have put

$$a = 1/\sqrt{\varepsilon\mu}\,, \qquad \sqrt{\beta^2+z^2} = \tau/\sqrt{\varepsilon\mu} = a\tau\,,$$

and $\phi_n(z, p)$ is the Laplace transform of $\phi_n(z, t)$ defined by:

$$\phi_n(z, t) = \begin{cases} 0 & \text{when } t<z/a\,, \\ J_0(k_n\sqrt{a^2t^2-z^2}) & \text{when } t\geqq z/a\,. \end{cases} \tag{4.4}$$

Thus, using this formula, we obtain the expression for $\Psi^{mz}(\vec{r}, t)$ in the form:

$$\Psi^{mz}(\vec{r}, t) = \frac{I_0\delta F}{2}\sum_n \frac{\psi_n(x_0, y_0)\psi_n(x, y)}{J(\psi_n)}\frac{1}{2\pi i}\int_{\alpha-i\infty}^{\alpha+i\infty}\frac{e^{-\gamma_n z}}{\gamma_n}\frac{e^{pt}}{p-i\omega}dp\,, \tag{4.5}$$

where $\alpha$ is the real part of $p$.

As usual, the above integral can be modified to a contour integral on the complex $p$ plane, the contour being taken to be the combination of a straight line $\alpha-i\infty \to \alpha+i\infty$ and a semicircle of radius $\infty$ on the right-hand or left-hand side, according as $t<z/a$ or $t>z/a$, as shown in Fig. 3. Let the Laplace transform and its inverse transform be designated by the operators $L$ and $L^{-1}$ respectively. Then we have

$$
\begin{aligned}
I_n &= \frac{1}{2\pi i}\int_{\alpha-i\infty}^{\alpha+i\infty} \frac{e^{-\gamma_n z}}{\gamma_n}\,\frac{I_0 e^{pt}}{p-i\omega}\,dp \\
&= aL^{-1}\{\phi_n(z,p)I(p)\} \\
&\quad - a\int_0^t I(t-\tau)\phi_n(z,\tau)\,d\tau \\
&= \begin{cases} 0 & \text{when } t<z/a, \\ I_0\int_{z/a}^t e^{i\omega(t-\tau)}J_0(k_n\sqrt{a^2\tau^2-z^2})\,d\tau & \text{when } t\geqq z/a. \end{cases}
\end{aligned}
\tag{4.6}
$$

Thus, we have finally

$$
\begin{aligned}
\Psi^{mz}(\vec{r},t) &= \frac{I_0\delta F}{2}\,a\sum_n{}'\frac{\psi_n(x_0,y_0)\psi_n(x,y)}{J(\psi_n)} \\
&\times \begin{cases} 0 & \text{when } t<z/a, \\ \int_{z/a}^t e^{i\omega(t-\tau)}J_0(k_n\sqrt{a^2\tau^2-z^2})\,d\tau & \text{when } t\geqq z/a. \end{cases}
\end{aligned}
\tag{4.7}
$$

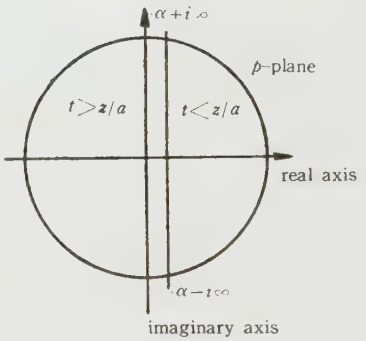


Fig. 3.

The above expression shows clearly that the electromagnetic waves propagate with speed $a=1/\sqrt{\varepsilon\mu}$ and that the phase velocity in the guide which appears in the steady-state solutions, is not the true propagation velocity.

The case (ii) in §3 can be treated in a similar manner. Only the final result is given here.

$$
\begin{aligned}
\Psi^{ez}(\vec{r},t) &= \frac{I_0\delta\zeta}{2\varepsilon}\sum_n{}'\frac{\varphi_n(x_0,y_0)\varphi_n(x,y)}{J(\varphi_n)}\,\frac{1}{2\pi i}\int_{\alpha-i\infty}^{\alpha+i\infty}\frac{e^{-\gamma_n' z}}{\gamma_n'}\,\frac{e^{pt}}{p(p-i\omega)}\,dp \\
&= \frac{I_0\delta\zeta}{2\varepsilon}\,a\sum_n{}'\frac{\varphi_n(x_0,y_0)\varphi_n(x,y)}{J(\varphi_n)} \\
&\times \begin{cases} 0 & \text{when } t<z/a, \\ \int_{z/a}^t \frac{2}{\omega}\sin\frac{\omega}{2}(t-\tau)e^{i\omega(t-\tau)/2}J_0(k_n'\sqrt{a^2\tau^2-z^2})\,d\tau & \text{when } t\geqq z/a. \end{cases}
\end{aligned}
\tag{4.8}
$$

Next, we shall discuss the behaviours of these expressions at $t\to\infty$, fixing $z$ at a finite value. We here consider only the case (i) in §3, since the other cases can be discussed similarly. Thus, by (4.7) we obtain

$$
\Psi^{mz}(\vec{r},t) = \frac{I_0\delta F}{2}\,a\sum_n{}'\frac{\psi_n(x_0,y_0)\psi_n(x,y)}{J(\psi_n)}\,e^{i\omega t}\int_{z/a}^t e^{-i\omega\tau}J_0(k_n\sqrt{a^2\tau^2-z^2})\,d\tau,
$$

where obviously $t>z/a$, since $t\to\infty$. Hence, using (4.3), we obtain

$$
\begin{aligned}
\Psi^{mz}(\vec{r},t) &= \frac{I_0\delta F}{2}\,a\sum_n{}'\frac{\psi_n(x_0,y_0)\psi_n(x,y)}{J(\psi_n)} \\
&\quad\times\lim_{t\to\infty}e^{i\omega t}\int_{z/a}^{\infty}e^{-i\omega\tau}J_0(k_n\sqrt{a^2\tau^2-z^2})\,d\tau \\
&\quad - \frac{I_0\delta F}{2}\sum_n{}'\frac{\psi_n(x_0,y_0)\psi_n(x,y)}{J(\psi_n)}\,\frac{e^{-\gamma_n z}}{\gamma_n}\lim_{t\to\infty}e^{i\omega t}.
\end{aligned}
$$

This is the steady-state solution, showing that (4.7) approaches the steady state as time increases.

## 5. Case 2 when the current $I_0$ begins to be impressed at $t=0$.

In case when $I(t)$ is a unit function, the expressions (4.7) and (4.8) in the preceding section are simplified. Thus, taking into account that when

$$\begin{aligned} I(t) &= 0 \qquad t<0 \\ &= 1 \qquad t\geqq 0\,, \end{aligned} \tag{5.1}$$

its Laplace transform is

$$I(p)=\frac{1}{p}\,, \tag{5.2}$$

we obtain the expression for this case by putting $\omega=0$, $I_0=1$ in the expressions in §4. Thus, for the case (i) in §3,

$$\begin{aligned} \Psi^{mz'}(\vec{r}, t) &= \frac{\delta F}{2}\, a \sum_n \frac{\psi_n(x_0, y_0)\psi_n(x, y)}{J(\psi_n)} \\ &\quad \times \begin{cases} 0 & \text{when } t<z/a\,, \\ \displaystyle\int_{z/a}^{t} J_0(k_n\sqrt{a^2\tau^2-z^2})\,d\tau & \text{when } t\geqq z/a\,, \end{cases} \end{aligned} \tag{5.3}$$

and for the case (ii) in §3,

$$\begin{aligned} \Phi^{ez'}(\vec{r}, t) &= \frac{\delta\zeta}{2\varepsilon}\sum_n \frac{\varphi_n(x_0, y_0)\varphi_n(x, y)}{J(\varphi_n)} \\ &\quad \begin{cases} 0 & \text{when } t<z/a\,, \\ \displaystyle\int_{z/a}^{t} (t-\tau)J_0(k'_n\sqrt{a^2\tau^2-z^2})\,d\tau & \text{when } t\geqq z/a\,. \end{cases} \end{aligned} \tag{5.4}$$

## 6. Case 3 when the impressed currents in cases 1 and 2 end at $t=T$.

In case when the space is excited by a rectangular pulse, the fields can be easily obtained from the above expressions. For example, in the case (i) in §3, the expression (5.3) is used to obtain

$$\Psi^{mz''}(\vec{r}, t)=\Psi^{mz'}(\vec{r}, t)-\Psi^{mz'}(\vec{r}, t-T)\,,$$

where $T$ is the duration of the pulse.

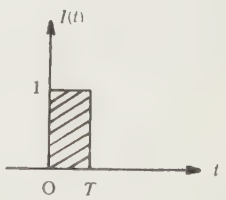

Fig. 4.

Hence,

$$\begin{aligned} \Psi^{mz''}(\vec{r}, t) &= \frac{\delta F}{2}\, a \sum_n \frac{\psi_n(x_0, y_0)\psi_n(x, y)}{J(\psi_n)} \\ &\quad \times \begin{cases} 0 & \text{when } t-T<t<z/a\,, \\ \displaystyle\int_{z/a}^{t} J_0(k_n\sqrt{a^2\tau^2-z^2})\,d\tau & \text{when } t-T<z/a<t\,, \\ \displaystyle\int_{t-T}^{t} J_0(k_n\sqrt{a^2\tau^2-z^2})\,d\tau & \text{when } z/a<t-T<t\,. \end{cases} \end{aligned} \tag{6.1}$$

The results for the other case can be obtained in a similar procedure.

Next, when the excitation is given by a harmonic wave train of finite duration, the formulae in § 4 are available. For example, in the case (i) in § 3, the expression (4.7) is used. Thus, if we put $I_0=1$ (say) in (4.7), we obtain

$$\begin{aligned}\Psi^{mz''}(\vec{r},t) &= \Psi^{mz}(\vec{r},t)-e^{i\omega T}\Psi^{mz}(\vec{r},t-T)\\ &= \frac{\delta F}{2}\,a\sum_n \frac{\psi_n(x_0,y_0)\psi_n(x,y)}{J(\psi_n)}\\ &\quad\times\begin{cases}0 & \text{when } t-T<t<z/a,\\ \displaystyle\int_{z/a}^{t} e^{i\omega(t-\tau)}J_0(k_n\sqrt{a^2\tau^2-z^2})\,d\tau & \text{when } t-T<z/a<t,\\ \displaystyle\int_{t-T}^{t} e^{i\omega(t-\tau)}J_0(k_n\sqrt{a^2\tau^2-z^2})\,d\tau & \text{when } z/a<t-T<t.\end{cases}\end{aligned}\tag{6.2}$$

## 7. The approximate formulae for the first precursors

While in the above sections we have obtained, by the use of Laplace transforms, the general solutions including the transient solutions, we shall discuss in this section the first precursors of the wave by Sommerfeld's method (**3**). We shall discuss the behaviours of $\Psi(\vec{r},t)$ and $\Phi(\vec{r},t)$. In order to obtain the electromagnetic field intensities, it is sufficient to differentiate them with respect to time and spatial coordinates. In this section, only the case considered in § 4, namely, the case where the impressed current $I_0e^{i\omega t}$ begins to be impressed at $t=0$ will be discussed.

(a) For the case (i) in § 3, we obtain, starting from (4.5),

$$\Psi^{mz}(\vec{r},t)=\frac{I_0\delta F}{2}\sum_n\frac{\psi_n(x_0,y_0)\psi_n(x,y)}{J(\psi_n)}\,\frac{1}{2\pi i}\int_{\alpha-i\infty}^{\alpha+i\infty}\frac{e^{-\gamma_n z}}{\gamma_n}\,\frac{e^{pt}}{p-i\omega}\,dp\,,\tag{7.1}$$

and

$$I_n^{mz}=\frac{1}{2\pi i}\int_{\alpha-i\infty}^{\alpha+i\infty}\frac{e^{-\gamma_n z}}{\gamma_n}\,\frac{e^{pt}}{p-i\omega}\,dp\,,\tag{7.2}$$

where, as before, $\gamma_n=(k_n^2+p^2\varepsilon\mu)^{1/2}$.

Now, if we put $p=i\omega'$, (7.2) becomes

$$I_n^{mz}=\frac{1}{2\pi i}\oint\frac{\exp\{i(\omega' t-\sqrt{\omega'^2\varepsilon\mu-k_n^2}\,z)\}}{i(\omega'-\omega)(\omega'^2\varepsilon\mu-k_n^2)^{1/2}}\,d\omega'.$$

The path of integration of the $\omega'$-plane is replaced by a circle of an infinitely large radius with its centre at the origin. Following Sommerfeld this circle is designated by U. As the measure of magnitude of the radius of U, the following may be adopted:

$$|\omega'|\gg \text{the larger of } \omega \text{ and } k_n/\sqrt{\varepsilon\mu}\,.\tag{A}$$

Hence, when $I_n^{mz}$ is computed, the following approximations are made:

$$\omega'-\omega\approx\omega',$$

$$(\omega'^2\varepsilon\mu-k_n^2)^{1/2}\approx\omega'\sqrt{\varepsilon\mu}\left\{1-\frac{1}{2}\frac{k_n^2}{(\omega'\sqrt{\varepsilon\mu})^2}\right\}.$$

Then we have

$$I_n^{mz}\approx-\frac{1}{2\pi\sqrt{\varepsilon\mu}}\oint\frac{e^{i(\omega't'+\xi_n/\omega')}}{\omega'^2}d\omega', \qquad (7.3)$$

where

$$t'=t-z\sqrt{\varepsilon\mu},\quad \xi_n=k_n^2z/2\sqrt{\varepsilon\mu}.$$

When we introduce a new integration variable $u$ such that

$$e^{iu}=\omega'\sqrt{\frac{t'}{\xi_n}}, \qquad (7.4)$$

we have

$$i\left(\omega't'-\frac{\xi_n}{\omega'}\right)=iu-it'\xi_n\left(\omega'\sqrt{\frac{t'}{\xi_n}}+\frac{1}{\omega'}\sqrt{\frac{\xi_n}{t'}}\right)$$
$$=2i\sqrt{t'\xi_n}\cos u-iu,$$

and therefore

$$I_n^{mz}\approx\frac{1}{2\pi i}\frac{1}{\sqrt{\varepsilon\mu}}\sqrt{\frac{t'}{\xi_n}}\int e^{2i\sqrt{t'\xi_n}\cos u-iu}\,du, \qquad (7.5)$$

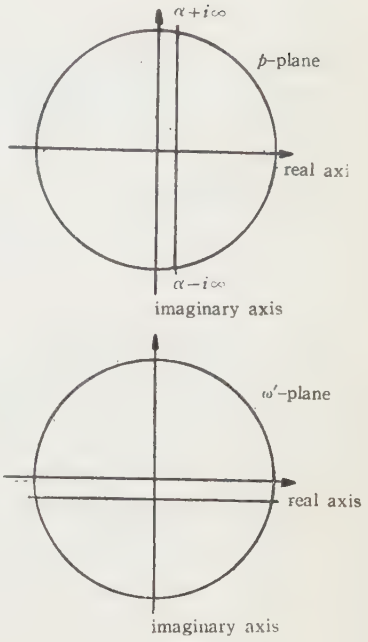

Fig. 5.

the integral being taken from $u=0$ to $u=2\pi$, since, as will be seen from (7.4), when $u$ varies from 0 to $2\pi$, a circle with its centre at the origin is described in the $\omega'$-plane. In case when $t'=t-z\sqrt{\varepsilon\mu}$ is sufficiently small, the radius of this circle satisfies the above-mentioned condition and so the approximation (7.5) is adequate. Therefore, when we take an adequately small $t'$, the approximate expression for $I_n^{mz}$ is

$$I_n^{mz}=\frac{1}{\sqrt{\varepsilon\mu}}\sqrt{\frac{t'}{\xi_n}}J_1(2\sqrt{t'\xi_n}). \qquad (7.6)$$

It is to be noted that since there are the condition (4) and the condition $k_n^2\leqq k_{n+1}^2$, the accuracy of the approximate formula (7.6) is different for various $n$ with the same $t'$. So this formula seems to be useful in order to discuss each mode individually.

(b) For the case (ii) in § 3, we have

$$\Phi^{ez}(\vec{r},t)=\frac{I_0\delta\zeta}{2\varepsilon}\sum_n\frac{\varphi_n(x_0,y_0)\varphi_n(x,y)}{J(\varphi_n)}I_n^{ez},$$
$$I_n^{ez}=\frac{1}{2\pi i}\int\frac{e^{-\gamma_n'z}}{\gamma_n'}\frac{e^{pt}}{p(p-i\omega)}dp \qquad (7.7)$$
$$\approx\frac{1}{\sqrt{\varepsilon\mu}}\frac{t'}{\xi_n'}J_2(2\sqrt{t'\xi_n'}),$$

where

$$t' = t - z\sqrt{\varepsilon\mu}, \qquad \xi'_n = \frac{1}{2}\frac{k'^2_n z}{\sqrt{\varepsilon\mu}}.$$

From these formulae the behaviours of the first precursors of electromagnetic waves can be investigated by differential operations.

**Acknowledgements**

The authors wish to thank Professors S. Tomotika for his helpful discussions.

REFERENCES

1. T. KIHARA, *Wave Guide* (in Japanese), Chap. 5, p. 83.
2. J. A. STRATTON, *Electromagnetic Theory*, p. 320.
3. A. SOMMERFELD, Die Fortpflanzung des Lichtes in dispergierenden Medien. Ann. d. Phys. **44** (1914), 201.

MEMOIRS OF THE COLLEGE OF SCIENCE, University of Kyoto, Series A,
Vol. XXVIII, No. 3, Article 3, 1957

# ON SOME RELATIONS BETWEEN ATMOSPHERIC IONS AND NATURAL RADIOACTIVITY

BY

**Sigeru OKABE**

(*Received July 30, 1957*)

ABSTRACT

The relations of atmospheric ions to atmospheric radioactive substances and to ground radioactivity were investigated by a direct measuring method. Namely, the height distribution of alpha-particles in the air near the ground surface was measured by a newly devised nuclear plate method, and the density of alpha-particles in the lower layer of the atmospheric ions to atmospheric radioactive substances was studied by an ion counter and an induction collector. The correlation between atmospheric ions and ground radioactivity in the spa was also studied and both correlations were ascertained to a certain degree and will be discussed here in some detail.

## 1. Introduction

It is commonly accepted that, in the lower layer of the atmosphere, the radiation of the radioactive substances that are contained in the air and in the uppermost stratum of the earth's crust is the principal source of atmospheric ion formation. This is an important fact in our research, as it determines to some extent the behaviour of the electric potential gradient and the conduction current at the point close to the ground surface. Recently, Cotton (**1**) studied these relations by means of a special ionization chamber. However, the relation between atmospheric ion and natural radioactivity has hitherto been treated only by a theoretical presumption based on some experimental data, and certainly no direct measurement of these correlations has ever been carried out. Therefore, it is considered to be important to make a suitable observation to ascertain the adaptability of the theoretical treatment and also study the reliability of the above-described correlations. And moreover, from these observations, some developments in this research field are anticipated. For instance, the abnormal intense radioactivity on the ground surface in the neighbourhood of hot springs (**2**) and the variation of atmospheric radioactivity connected with an earthquake (**3**), which were already reported in this Memoir by the present writer, may more clearly be interpreted in connection with atmospheric ions. Concomitantly, the work by Ito (**4**) intending to clarify the luminous phenomena from the side of correlation of earthquake with ground- and air-radioactivity, is considered to be, anew, highly appreciated. In this paper, the results obtained by some direct measurements

to study the relation between atmospheric ions and ground- or air-radioactivity, are reported in some detail.

## 2. Distribution of alpha-particles in the atmosphere

As the alpha-particle is the main ionization source of atmospheric ions, and moreover the distribution of radioactive elements in the air is also ascertainable by alpha-particles, measurement of the distribution of alpha-particles is considered to be highly important in the investigation of the relation between natural radioactivity and atmospheric ions. But, no practical, detailed measurement has yet been carried out on these problems, though there are some theoretical calculations by Priebsch (**5**) and the finding by Hess (**7**) based on the theory of Schmidt (**6**) and Priebsch. There are some possible methods to measure directly alpha-particles in the air. Namely, a method of measuring alpha-particles in the air directly by using a scintillation counter, a method of using some vacuum large ionization chamber into which is introduced a sample of air containing radioactive elements, a method of using a nuclear plate as a detector of alpha-particles, and others, are practicable ones. After comparing the advantages of these different methods, the nuclear-plate method was employed in preference to the others, in the present research. Throughout the following investigation, a newly devised nuclear plate camera with some accessories was utilized; and the distribution of alpha-particles in the air as observed with this equipment will be described. Observation was then carried out by means of the newly devised nuclear-plate camera with its accessories, and consequently, distribution of alpha-particles was studied.

### *2.1 Apparatus and method of measurement*

Most of the radioactive substances in the air are Radon, Thoron, and their decay products (**8**) (**3**), and the artificial radioactive products as developed to the present are quantitatively negligible compared with natural ones. As an example, a part of the results of a continuous measurement of atmospheric radioactive substances conducted at a point one meter above the ground surface on the playground of Tottori University, in Tottori city, is shown in Fig. 1, and a comparatively large irregular variation is clearly observed. Cotton (**1**) describes in his report that this sort of variation is related to the turbulent exchange in the air adjacent to the ground surface. However, it is rightly interpreted from the observational result previously obtained by the writer (**3**) that this variation is mainly related to the difference of Radon content in different air masses. Moreover, it was found from the present observation by a nuclear plate method that the number of tracks observed of alpha-particles is extremely small, namely, being 1 track/cc/scores of hours. For these reasons, these sorts of

observations should be continued over a fairly long period to avoid statistical errors and to obtain adequate proof.

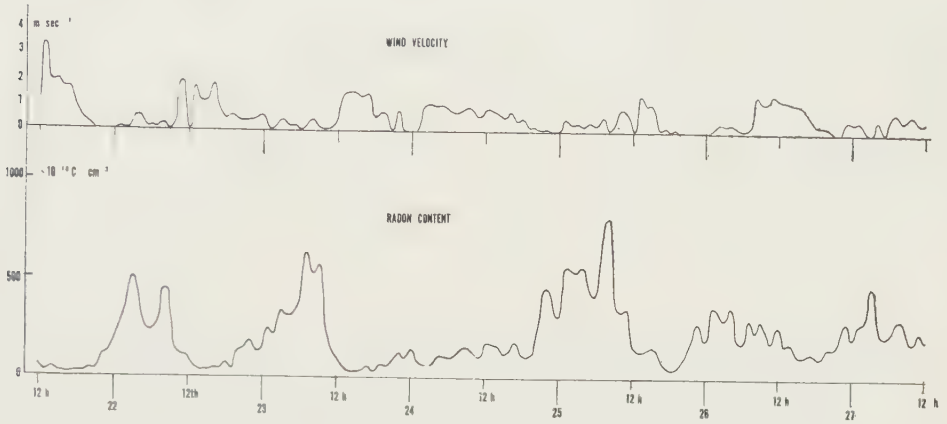


Fig. 1. Atmospheric radon content and wind velocity (July, 1956).

The apparatus and its practical manipulation in measurement are briefly described as follows: six camera-boxes, each size being $13 \times 12 \times 6$ cm, are jointed together into a single unit and the camera cover is loaded with six nuclear plates in its interior, the end of the air-introducing rubber tube on one side of each camera being kept at a suitable height, while the tube on the other side is connected to an aspirator-pump. An adjusting valve for keeping the air flow of same amount, and a light-interception plate are fixed at the connection point of rubber tube and camera box as schematically shown in an arrangement-diagram of Fig. 2. The power of the aspirator-pump is adjusted to 180 L/hour to prevent the disturbance of air at the pipe entrance, and the pump-motor is so arranged as to be operated by battery for portable purposes. First,

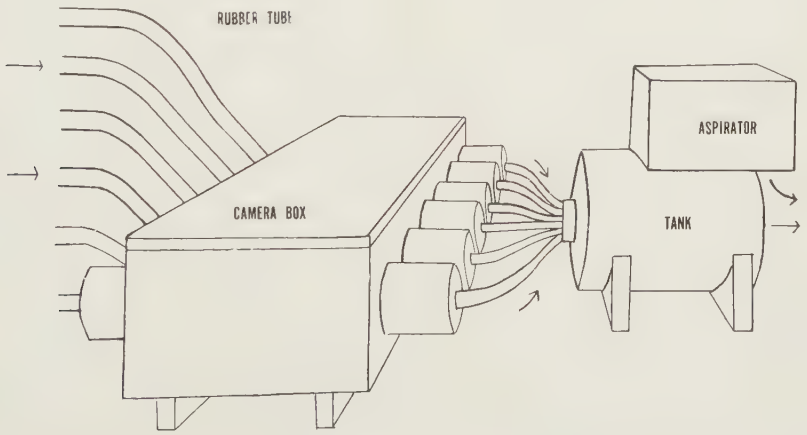


Fig. 2. Arrangement of nuclear plate camera and aspirator.

the camera was loaded with a nuclear plate, each rubber tube was supported at a suitable height, and then the aspirator-pump was operated for a period of 3～10 hours. The exposed nuclear plates were then developed as soon as possible after exposure. The number of alpha-particle tracks on 100 numbers of field of view by ×400–microscope were counted and the radius of each field was found to be 230 $\mu$. (see Fig. 3) The nuclear plates "Sakura" were chiefly employed in the present observation, its emulsion thickness being 50 $\mu$. In practical measurement, the effect caused by any disturbing radioactivity superposed upon the properly aimed radioactivity is appropriately corrected by comparing the exposed plate in the above-described treatment with the unexposed one.

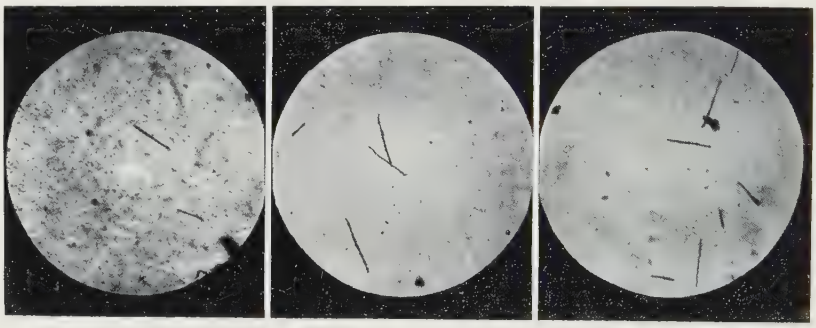

Fig. 3. Some examples of $\alpha$–particle track observed by nuclear plate. (×600)

*2.2 Results*

Considering the various conditions stated in the introduction, measurement was carried out at the plain, rice field, wood and spa, both in the daytime and at night. The results of observation are shown in Fig. 4, the ratio of each value obtained to the mean value is plotted for the benefit of comparing the relative distribution of alpha-particle with height. In Fig. 5, the sum of all data obtained during the 104 hours are shown without any consideration on any conditions concerning the observed place, weather, and other conditions ; therefore it may safely be said that it shows the mean tendency of the distribution of alpha-particles. In this measurement some disturbing effects must be taken into consideration ; such as the attachment of emanation, the inequality in the balance of radioactive equilibrium of the aspirated elements, and others. Moreover, as the number of tracks of alpha-particles which is registered on the nuclear plate shows some parts of total particles that are radiated in the camera box, it seems difficult to get an accurate, absolute value of height distribution of alpha-particles and radioactive elements by this method. From these reasons, the argument in the present research is reasonably restricted to the problem on relative correlation of intensity of alpha-particles with height.

In this measurement it was found that the sample air needs about 20 seconds to pass through the rubber tube, and therefore, considering the decay process of the radioactive substances, the results obtained should be interpreted as the intensity of alpha-particles measured at any level showing in reality a level higher than the height of the rubber tube-end. These level corrections are tentatively calculated after the theoretical treatment of Priebsch (**5**), and are as follows; for example, the height above the ground surface of 10 cm is corrected as 20 cm, 55 cm as 100 cm, 95 cm as 150 cm, and 200 cm as 310 cm respectively. But these corrections themselves need to be examined, because, the theoretical results by Priebsch and Hess of the alpha-particle distribution at the ground level, for example, are twice as large as those at the height of one meter, and are not in agreement with the practical measurement, as shown in Figs. 4 and 5. Though it is difficult, under such circumstances as above described, to obtain a definite conclusion concerning the height distribution of the emanation, it may possibly be said, from the present measurement, that the distribution-intensity of alpha-particles is comparatively

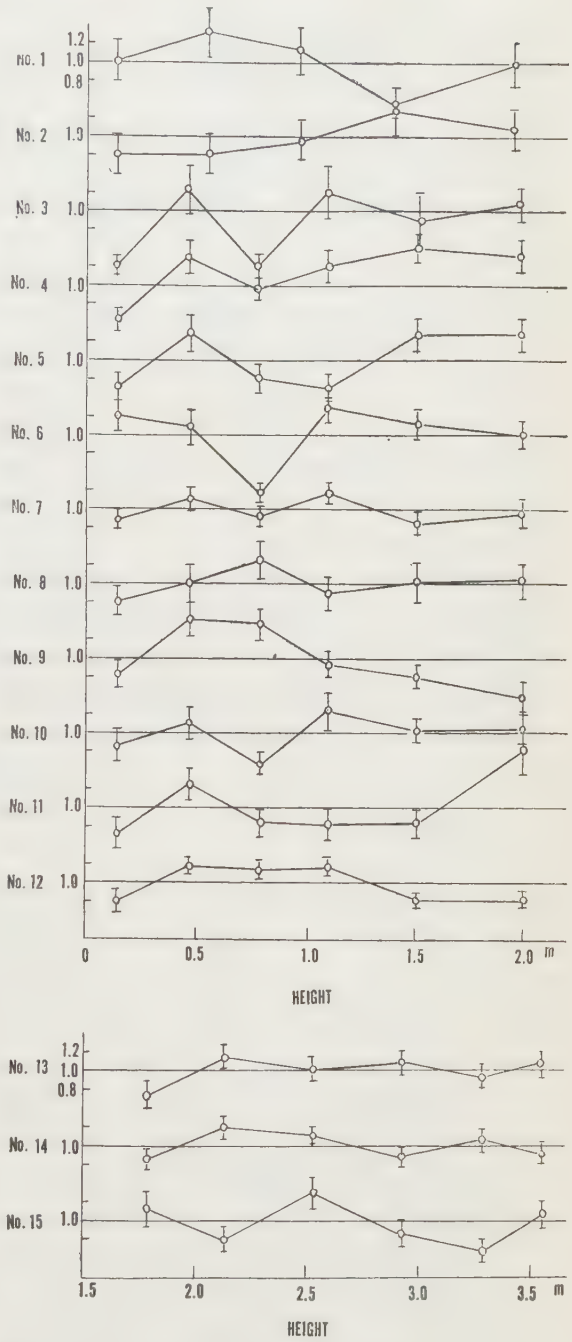


Fig. 4. Ratio of distribution of alpha-particles. Nos. 1, 4, 5: at play ground; No. 2: at valley of cypress; No. 3: at spa; Nos. 6, 7, 10, 11, 12, 13, 14, 15: at rice field; Nos. 8, 9: at bamboo grove.

small at the ground level, and large at 0.5 meter-height, and, from the level of 1.0 m up to 4.0 m, a certain fluctuation is observed with a range of less than 20% of the value at 1.0 meter-height.

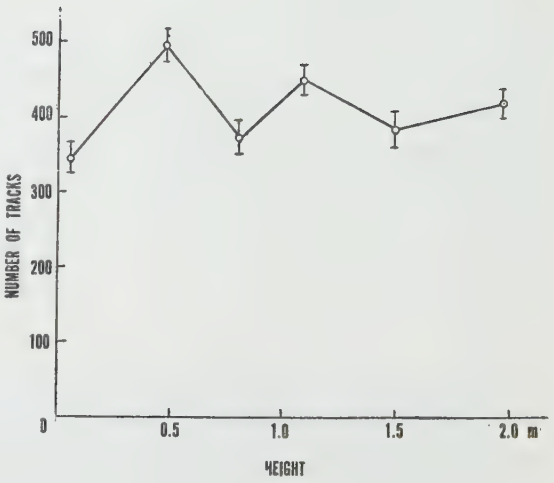


Fig. 5. Height distribution of alpha-particles.

### 3. The relation between atmospheric small ion and radioactive elements in the air

The diurnal variations in atmospheric radioactivity have been investigated at many locations throughout the world since the first observations in the early 1900. Also the continuous observations on the rate of ionization have been carried out at some stations, and the curves of their diurnal variations have been expected to show the same form. But, since the process of formation and destruction of small ions is too complicated, the relation between atmospheric radioactivity and atmospheric ions have not yet been investigated. Namely, the process of combination of small ions with condensation nuclei, the mingling with the ions formed at other places, the recombination with those of opposite signs, and other conditions are very complicated. However, it is quite interesting and essential in the research branch of atmospheric electricity to study whether or not there exists a certain correlation between atmospheric small ions and atmospheric radioactivity in the open field.

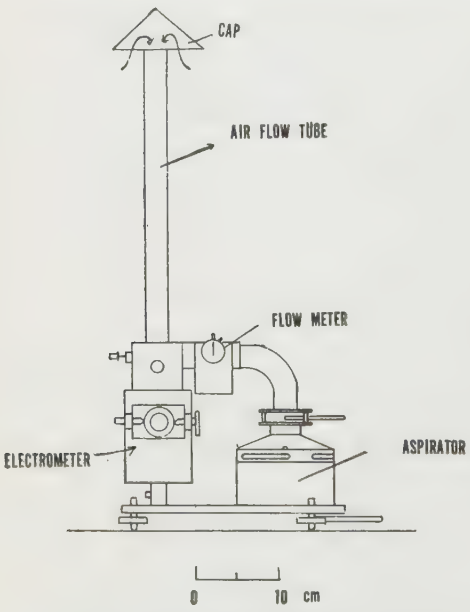


Fig. 6. Ebert ion counter with Wulf electrometer, No. 6191.

*3.1 Apparatus and some considerations*

(a) Apparatus for ion measurement

For the measurement of atmospheric small ions, a portable ion counter has been used, its construction is shown in Fig. 6. The essential features are, as seen in the figure, the air flow tube, the

Wulf-type bifilar electrometer, the anemometer connected at the base of the air flow tube, and the cylinder at the right-hand side of the electrometer in which is contained a spring-driven air flow fan. The cap on the top of air flow tube is equipped with a screen through which the air is inhaled into the counter.

The method of measurement is as follows: the fiber of bifilar electrometer was charged by a dry cell of 90 volts, operating the aspirator for five minutes, and then the number $N$ of an anemometer was read. From the reading difference of division $(V_0 - V_t)$ of the electrometer, $V_0$ and $V_t$ being the scale readings at the time of initial charge and at any time $t$ after the initial charge respectively, the charged electricity in the central collector is given by an expression in the formula

$$E = \frac{16.18 \cdot (V_0 - V_t)}{N \cdot 1.16 \cdot 10^3 \cdot 300}. \quad \text{(c.g.s. esu)} \qquad (1)$$

Supposing that each small ion has an elementary charge, the number of ions in the aspirated air, is given as follows:

$$n = E/4.8 \times 10^{-10}.$$

In some observations a vinyl pipe of 2 meters' length and 2 cm radius was connected to the air flow tube, for collecting the sample air at a higher level. In this case, not only the mass of inflowing air is decreased by the resistance of the vinyl tube, but an excess attachment of the ions to the inner wall of the tube is feared. Fig. 7 shows the result which was obtained by operating an ion counter attached to the vinyl pipe, when X-rays of known intensity were radiated to several different points on the vinyl pipe. But the existing condition of naturally small ions is so complicated that any regularity in the decrease in height cannot be expected in this case. Therefore the formula (1) cannot be applied in these cases and it is safely understood that the observed value shows only a relative correlation.

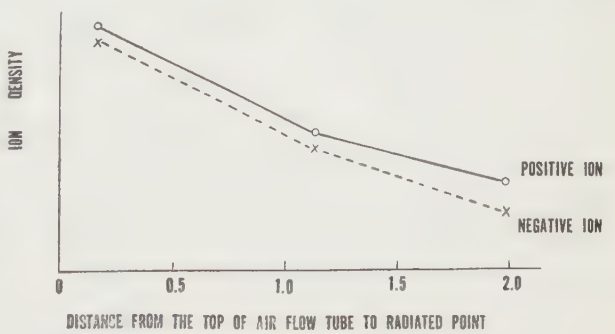


Fig. 7. Decrease of the flowing ions when vinyl pipe is connected.

(b) Collecting apparatus of atmospheric radioactive elements

The filter paper method is a well-known method for collecting atmospheric radioactive elements, but it has poor efficiency compared with the other two methods which will be described here (8) (9). Namely, the improved induction-method, and the corona-discharge method were employed in the present measurement. For the purpose

of comparing the corona-discharge method with the induction method, the former was investigated with high voltage, 12 KV, similarly used by Wikening (**10**). It is ascertained by this experiment that the efficiency of the two methods for collecting atmospheric radioactive elements is nearly equal, and though the induction method can be expected to collect RaA and ThA, the corona-discharge method, on the contrary, cannot catch the positive charged elements. For instance, in studying the typical decay-curves plotted from the deposits of the two methods, the corona-discharge method shows considerably less uniformity in its shape compared with the curves of the induction method. Consequently, the improved induction method is more advantageously adopted than that of corona-discharge for the present research.

As the details of the improved induction method were already reported by the writer in this Memoir (**3**), only a simple description will be given here. Air of 2.0 $m^3$/minute is aspirated through the air tube of a 14 cm radius, and the metal plate charged with the negative high voltage of 11 KV, is hung in the centre of the tube; then the atmospheric radioactive elements and their decay products will be caught to that metal plate. After a 30-minute hanging of the metal plate, it is measured with the Lauritsen electrometer. The value of measurement expressed as d.p.m. (scale division per minute) shows the mean value of change in scale-division per 10 minutes in the present observations. The efficiency of this measurement was about 3% as examined with a known quantity of Radon. The amount of Thoron and its decay products are assumed to be comparative to that of the atmospheric Radon content.

(c) The effect of the electric field

At the location of the ion counter, it is considered that the apparatus is grounded through the body of the observer and a stand, and then the intensity of the electric potential gradient may be large at the top of the air flow tube. The influence of the electric field on the efficiency of the ion counter will be examined. Fig. 6 shows the arrangement used for this research. The area of the electrode plates which are used to make an artificial electric field is $3 \times 2$ m, and they are separated 1 meter apart from each other, X-ray being used as an ion source in this case. According to the results of measurement, as shown in Figs. 8 and 9, it may be said that the influence of the electric field is negligible so far

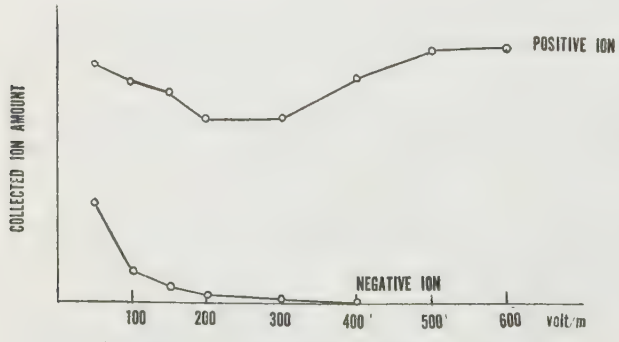

Fig. 8. Effect of the artificial negative electric field.

as the measurement of positive ions is concerned, because, in a normal condition, the potential gradient is about negative 100 volt/m. And as it is considered that the small ions which are made by X-rays have larger mobility than out-door small ions, the above-mentioned effect becomes increasingly negligible. Consequently, the measurement of the electric field was not made in these observations, but the observations were carried out at as unobstructed a place as possible to avoid any change of electric field influenced by some object as has been mentioned by Ishikawa (**12**).

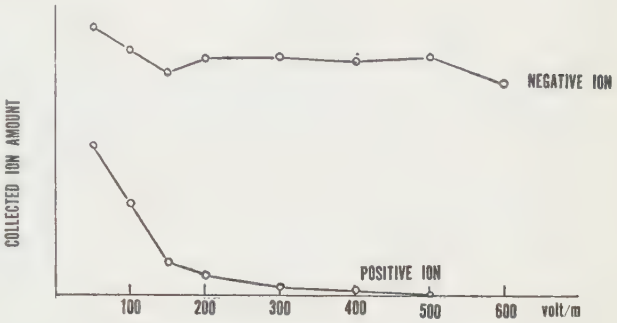

Fig. 9. Effect of the artificial positive electric field.

*3.2 Measurement and results*

(a) On the electrode effect

Hogg (**13**) and other researchers have reported that the potential gradient on a day of fair weather decreases with height in an area of few meters above the ground surface owing to a depletion of the negative ions in that area. This is the so-called electrode effect. The phenomenon is explained by the negative ions drift away from the earth due to the action of the electric field, and the concentration of the negative ions becomes small at the point close to the surface.

The influence of this phenomenon on the relation between atmospheric ions and radioactivity, in other words, on the relation between the height of the aspiration tube and the type of ions concerned, was studied in the present measurement, by connecting the vinyl pipe to the top of the air flow tube. According to ten preliminary observations, in cases where wind velocity ranged from 0 to 2 m/sec, no influence of electrode effect was observed as shown in Fig. 10 and Figs. 13, 14, 15, and also, with regard to the amount of positive or negative ions no difference was observed, as shown in Figs. 11, and 12. But so far as these observations are concerned, atmospheric radioactive substances and ions seem to have some correlation, and

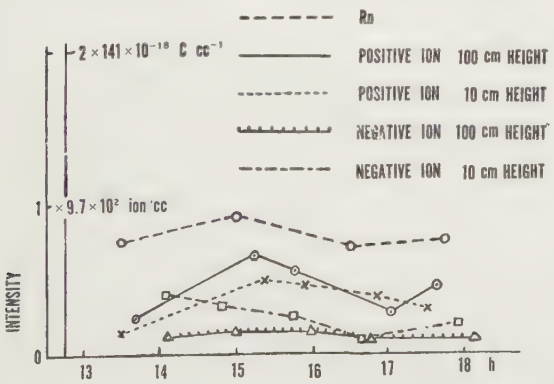

Fig. 10. Height distribution and time variation of ions.

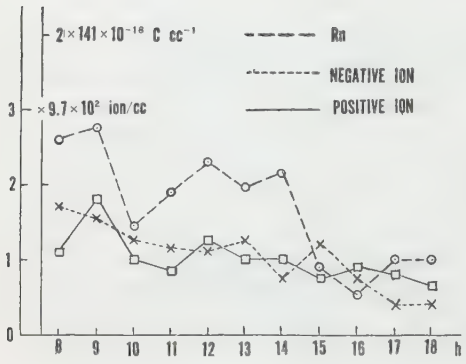


Fig. 11. Time variation of ions.

these results are fairly reasonable. From the above-mentioned reason, positive small ions are expected to be chiefly observed in the present case. Considering these phenomena of Fig. 10, the height of the cap of the air flow tube of the ion counter is profitably arranged at the level of 1～1.5 meters.

(b) Results of the measurements

The measurement concerned was carried out at the play ground of Tottori University, and its condition are described in another report by the writer (**3**).

It is to be remarked that the data on rainy days are very scanty because the portable ion counter cannot be operated during rain. To investigate the results of Cotton (**1**), each datum was correspondingly compensated to the wind velocity observed at that time. In all of these measurements those data on which significant diural effects were observed are selected and explained here. The intensity of atmospheric radioactivity means the radioactivity of the substances which have been deposited on the collector-plate for the induction method during an interval of 30 minutes. The ion counter was operated for five minutes during the observation. The main wind directions are shown in Figs. 12～19. Fig. 12 shows the special data on September 9, 1956, when Typhoon No. 12 was passing near the place of observation. In this figure, no general nature of the diurnal variation, and no correlation between the

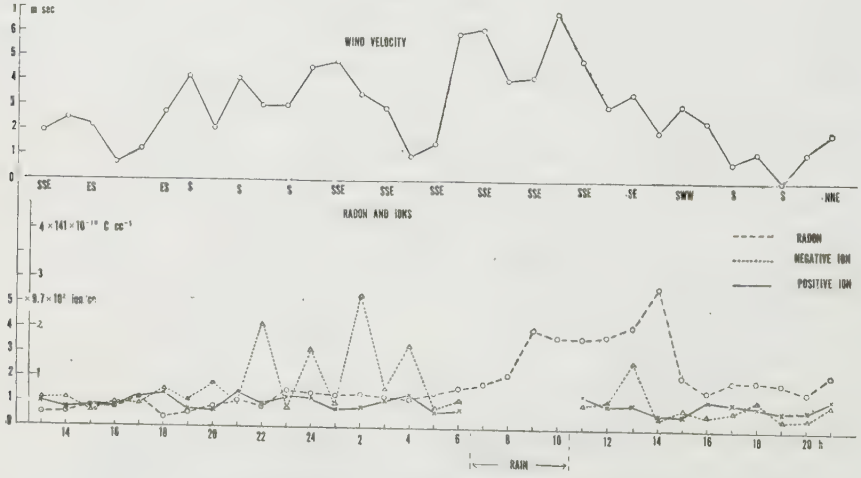


Fig. 12. Diurnal variation of ion, Radon and wind velocity on September 9～10, 1956.

atmospheric ions and radioactivity can be detected, consequently the argument by (**1**), namely the relation between wind velocity and atmospheric radioactivity is not demonstrated from the data in Fig. 12. Fig. 13 shows the data on November 18, 1956, as an illustration of data on a calm cloudy day. In it a certain correlation between atmospheric ions and radioactivity is detected especially in the data of 10 cm height from the ground surface. Any definite relation of wind velocity to Radon cannot be observed here, too. Fig. 14 shows the data on November 21, 1956, when the mean cloud

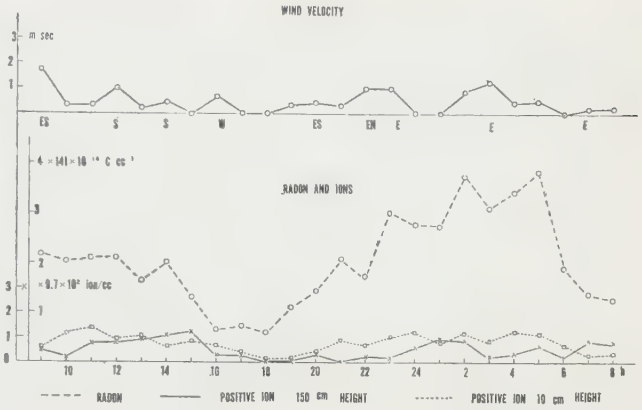


Fig. 13. Diurnal variation of ion, Radon and wind velocity on November 18~19, 1956.

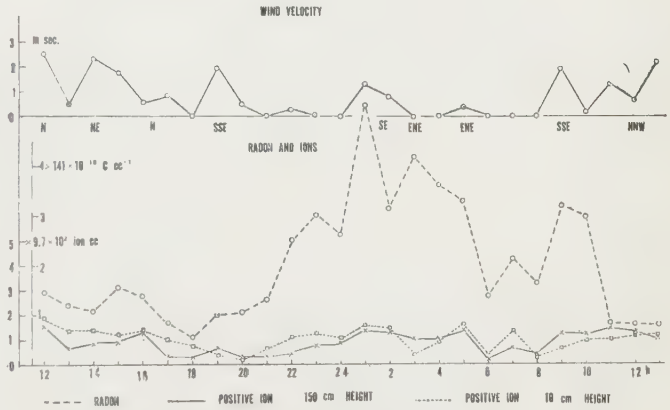


Fig. 14. Diurnal variation of ion, Radon and wind velocity on November 21~22, 1956.

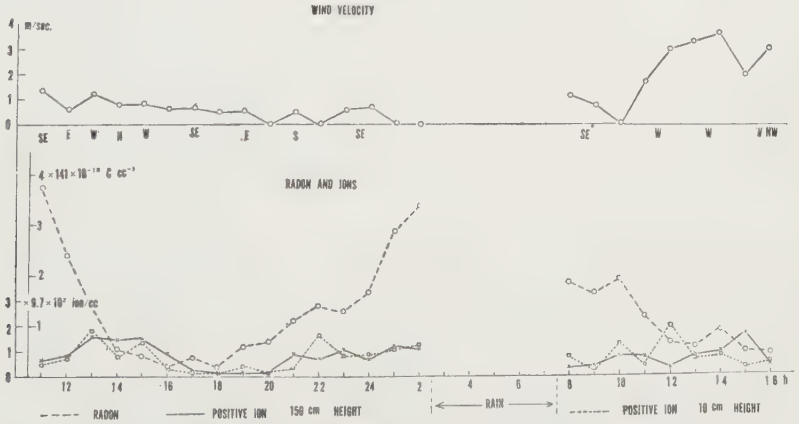


Fig. 15. Diurnal variation of ion, Radon and wind velocity on November 28~29, 1956.

quantity is half and the weather is fine. The correlation between ions and radioactivity seems to exist in some degree in this figure, being clearly observed particularly at about 18 h and 6 h, while, on the other hand, the relation of wind velocity to Radon is neither observed here, nor in Fig. 12.

Fig. 15 shows the data on November 28 and 29, 1956, when it rained from 2 h to 8 h on the 29th. It exemplifies the data observed before and after the rain. From the graph of 11 h to 16 h on the 28th and 9 h–11 h on the 29th, no correlation is observed. The relation of wind velocity to Radon is also negative in this case.

Fig. 16 shows the data on April 7, 1957, when the cloud quantity was 0 and fine weather lasted for about three days. The chart's curve is similar to that in Figs. 13 and 14 and, the correlation of ions to Radon is most clearly observed. Fig. 17 shows the data on April 13, 1957, when the cloud quantity was 0. Here, the correlation of wind velocity to Radon is fairly good, but the correlation of Radon content to ions is rather less; especially in the variation at 19 h–22 h and 7 h–9 h. Fig. 18 shows the data on April 26, 1957, when it had been raining heavily for three days just before the beginning of the observation. The play ground was covered with a sheet of water throughout the 26th; therefore, the ions which are generated at the ground surface by alpha-particles and beta-particles, are considered to have been greatly decreased. In this figure, the maximum atmospheric ions seem to be partially correlated with the Radon content, and

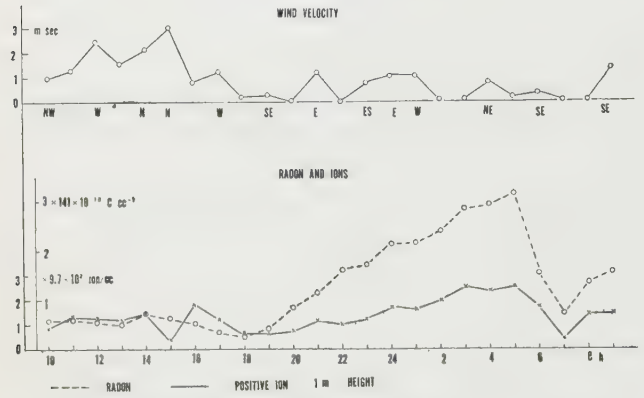


Fig. 16. Diurnal variation of ion, Radon and wind velocity on April 7~8, 1957.

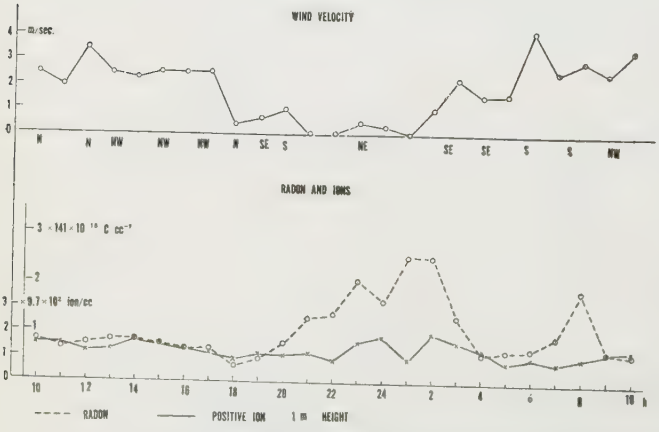


Fig. 17. Diurnal variation of ion, Radon and wind velocity on April 13~14, 1957.

its reason may possibly be attributable to the extinction of disturbing effect caused by ground activity which was greatly reduced by the cover of water sheet on the ground. Fig. 19 shows the data on May 9, 1957, when the cloud quantity was 0. It is an illustration of the atmospheric radioactive substances during the daytime which are considerably larger as in Fig. 13.

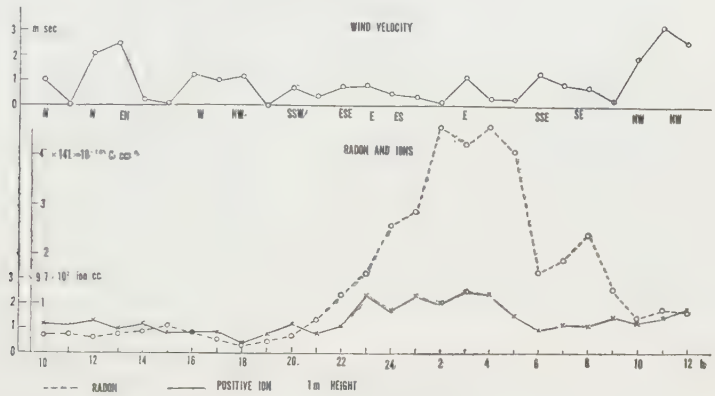


Fig. 18. Diurnal variation of ion, Radon and wind velocity on April 26~27 1957.

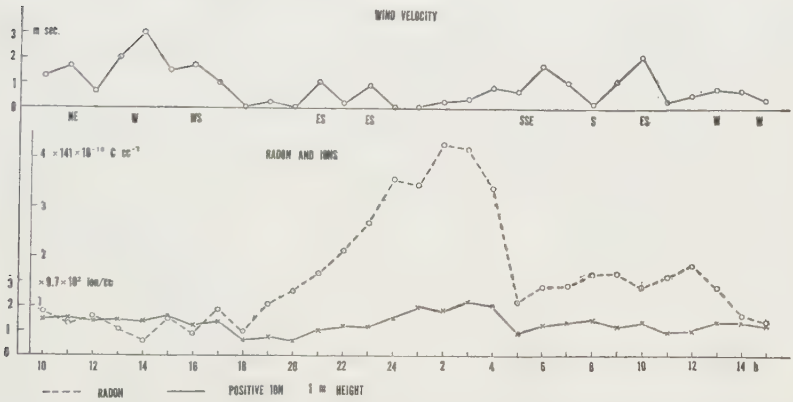


Fig. 19. Diuanal variation of ion, Radon and wind velocity on May 9~10, 1957.

(c) Conclusion and discussion

The process of ion formation is balanced by the process of ion destruction. The equation of ion balance was studied by Gish (**14**), and, under a suitable assumption, it is written as

$$q = 2\eta nN,$$

where $q$ is the formation of small ions (expressed in ion pairs per cc per sec), $\eta$ is the combination coefficient, $n$ is the concentration of small ions (in ions per cc) and

$N$ is the concentration of large ions. Therefore, if changes in $q$ are neglected, the value of $n$ is inversely proportional to $N$. The relation has been confirmed by several experiments, and it is an important condition which must be considered at present. The average value of ionization of the atmosphere, at one meter above the earth's surface, has been estimated lately by Hess (**15**) at about 7.3 ion pairs per cc par sec. The detail is as follows; 1.76 ion pairs generated by alpha-particles; 0.40 ion pairs by beta-particles; 3.15 ion pairs by gamma-rays; 1.76 ion pairs by cosmic radiation. According to this, the value of ionization by the atmospheric radioactive substances, may be estimated to be about 2 ion pairs. On the other hand, Hess (**19**) reports that, if the mean coefficient $A$ of eddy diffusion at a point between 10 and 100 cm above the ground is assumed to be $0.5\,\mathrm{cm^{-1}\,g\,sec^{-1}}$, the contribution of small ions produced by alpha-particles near the ground to the total ion content at one meter from the ground (about 200~600 small ions per $\mathrm{cm^3}$) may be generally rather small (about 5–10 per cent). Therefore, the rate of ionization of the atmospheric source can be written as:

$$(1-0.1)\times\frac{2}{7.3}\simeq 0.25\,.$$

This rate may change with the variation of the atmospheric conditions. In addition to this, it must be considered that a part of the measured small ions have travelled, being reduced along the path from other places to observation point, under the effect of electric field, eddy diffusion and density of neutral condensation nuclei. The process of collision of a small ion with a neutral condensation nucleus is also important.

From the above-mentioned consideration, the rate of atmospheric ions that are originated from atmospheric radioactive substances, seems to be about 20–10 per cent.

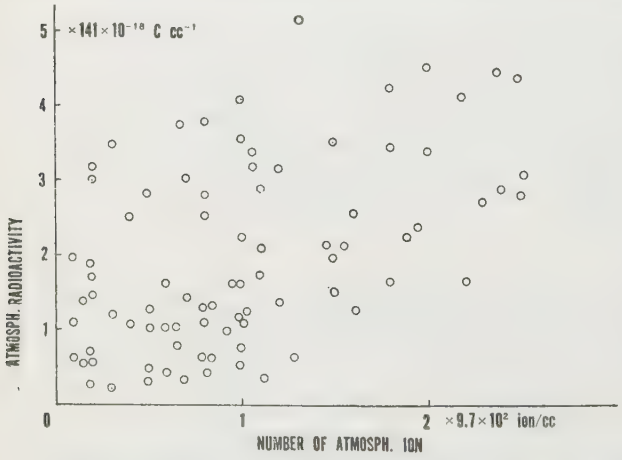


Fig. 20. Relation between atmospheric radioactivity and number of atmospheric ion at night.

Conversely, according to the observation in this research which was carried out during August 1956~May 1957, the relation between atmospheric ions and atmospheric radioactive substances is vague, as is shown in Figs. 11~18. Namely, the times when the atmospheric radioactivity and atmospheric ions show minimum values seem to coincide with one another in most cases, while

the maximum value of positive small ion density at midnight is almost equal to the value during the daytime, in spite of the fact that the atmospheric radioactivity at midnight is about 5～10 times as large as that in the daytime. But, when the nighttime and daytime data are classified and arranged in a proper order, as shown in Figs. 20～23, the correlation seems to be fairly better at nighttime. Fig. 22 shows that 0～80% of atmospheric ions at night originates from atmospheric radioactive substances under the condition of Fig. 19. This phenomenon cannot be explained only by Austausch effect, and the correlation is considered to be certainly accidental.

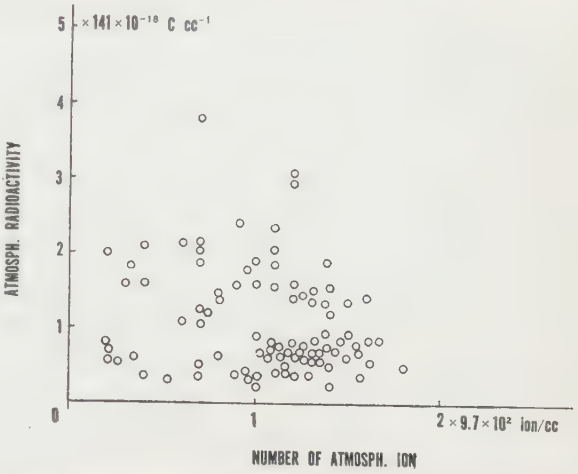


Fig. 21. Relation between atmospheric radioactivity and number of atmospheric ion at daytime.

Therefore, in consideration of this correlation, the possibility of appearance of the luminous phenomena which were often reported as following a destructive earthquake being explained by the increased atmospheric ions originated from the atmospheric radioactive substances following an earthquake, is concluded to be rather questionable.

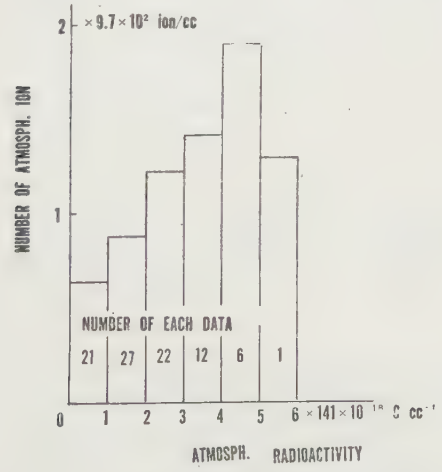


Fig. 22. Relation between atmospheric radioactive substances and ion density at night.

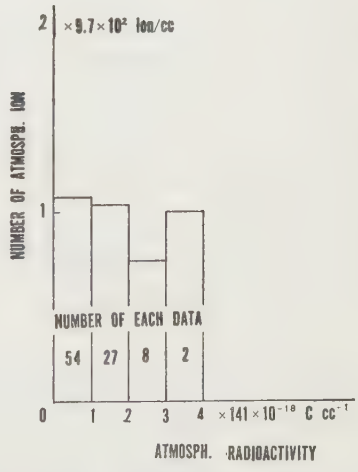


Fig. 23. Relation between atmospheric radioactive substances and ion density at daytime.

**4. Relation between atmospheric positive small ions and ground radioactivity**

The intensity of radioactivity on the ground surface is generally explained mainly to be influenced by the soil at that point, and especially, marked by the existence of the faults or hot springs.

Recently, Giletti (**17**) carried out some researches on the Radon leakage from radioactive minerals and Hatsuda (**18**) carried out researches on the intense radioactivity at the fault, and also the present writer investigated the intense radioactivity at the spa (**1**). Also, the writer has recently reported some correlation between electric potential gradient and the intensity of ground radioactivity at a spa (**19**). An abnormal space-charge density at the spa is, as a natural consequence, expected from these results. Therefore, the existence of a correlation between atmospheric small ions and ground radioactivity is also reasonably expected. Such correlation will be studied at several places.

*4.1 Apparatus and method of observation*

(a) Measurement of ground surface radioactivity

For the measurement of ground surface radioactivity a portable Geiger-Müller counter set called 2S–Pl was used, which was reconstructed so as to make it possible to connect two G–M counter tubes at the same time to meet the requirement of the present investigation. The details of this method of measurement were already described in another report by the writer (**2**), and will be mentioned briefly here. The natural counts of the 2S–Pl, which connect two G–M counters, are about 60–80 c.p.m., the counters being operated by dry cells. The end-window type counter which was used here, has a mica-window of 2 mg/cm$^2$, and is covered with 90 mg/cm$^2$ aluminium plate. The counter is supported 15 cm above the ground surface by a suitable stand. With this apparatus gamma-rays and a part of beta-rays are measurable, but it is assumed here that all radioactive radiation from the ground surface is proportional to the reading of the recorder.

(b) Measurement of ions

For the measurement of atmospheric ions, a portable ion-counter that is described in 3.1 (a), was used, and the height of the air flow tube was adjusted just one meter above the ground surface.

*4.2 Measurement and results*

Measurement was carried out simultaneously with an ion counter and a G–M counter at the same point for a duration of five minutes. Those days were selected when wind velocity was less than one meter and the weather was fine, because the area of abnormal radioactivity was relatively small as it was necessary to avoid the effects from an electric field produced by clouds. In a locality measurement, 3~6

hours are needed.

Assuming that the diurnal variation in the measured area is equal, the effect of diurnal variation is avoided by correcting the data obtained at the different points, compared with the diurnal variations observed after every three observations at the same fixed point.

Certainly, this amendment is not considered to be perfect but it seems to be rather conclusive in the present treatment. A preliminary observation was carried out to decide which observation would show a better correlation, an observation at nighttime or daytime. For several tests above mentioned, it was decided that all observations should favourably be carried out in the daytime.

The corrected results of measurement are shown in Figs. 24～28, and the map of each place has already been printed in the other reports by the writer (**2**).

Fig. 24 shows the observation at the Iwai hot spring and a. b. c. ··· denote the measured points. The geological formation at Iwai hot spring is a complex of tertiary tuff, shale and sandstone, and the Radon content in the thermal water is 1 Mache. The ground radioactivity measured by G-M counter is about 70～90 c.p.m.. This measurement was carried out between 9h～13h, when there was no wind and the weather was fine. The correlation coefficient between the atmospheric small positive ion density and the ground radioactivity is calculated as $r=0.50$. To illustrate the reason why the measurement was carried out in the daytime, two cases of measurement conducted in the afternoon and at midnight should be mentioned here. The correlation coefficient in the afternoon when the wind velocity was rather large, was $r=0.43$, and that at night on the same day was $r=0.27$.

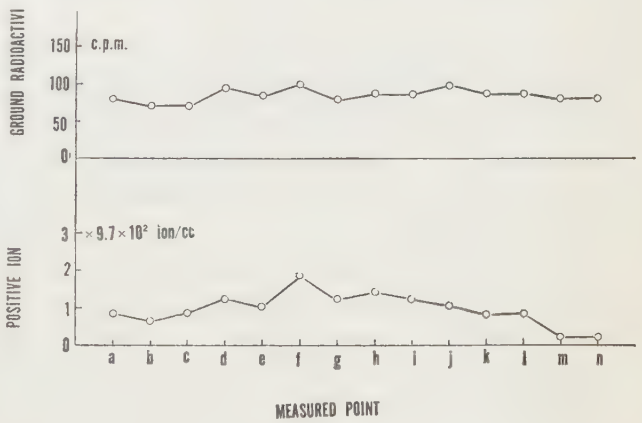


Fig. 24. Ground radioactivity and number of positive ion observed at Iwai hot spring.

Fig. 25 shows the observation at the Misasa hot spring. The bed rock of this area is porphyritic granite and it is intruded in spots by the fine grained granite, from where thermal water springs out. The Radon content of the thermal water is about 100 Mache and the Radium content of this region is large. The ground radioactivity measured by G-M counter is about 90～110 c.p.m.. The observation was carried

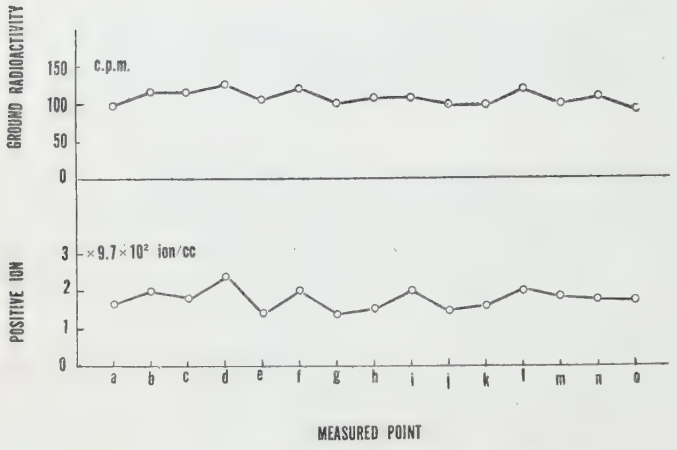


Fig. 25. Ground radioactivity and number of positive ion observed at Misasa hot spring.

out between 11h and 15h, when the wind velocity was almost 1m/sec and the weather was fine. The correlation coefficient between atmospheric small positive ions and ground radioactivity is calculated as $r=0.65$. It is supposed that, if the wind velocity of that day had been smaller, the correlation might have become larger.

Fig. 26 shows the observation at the Hamamura hot spring. The bed rock of this region is formed by strongly radioactive granite and the ground surface is an alluvium area with alternating strata of clay-beds and gravel. This locality is surrounded by sand hills and rice fields. The Radon content in the thermal water is several Mache, and the ground radioactivity measured by G-M counter is about 70～100 c.p.m.. The measurement was carried out from 9h to 14h, when it was cloudy with no wind. The correlation coefficient between atmospheric small positive ions and ground radioactivity is calculated as $r=0.52$.

Fig. 27 shows the observation at the Togo hot spring. This locality is situated close to the southern part of the small Togo Lake, and its bed rock is granite covered

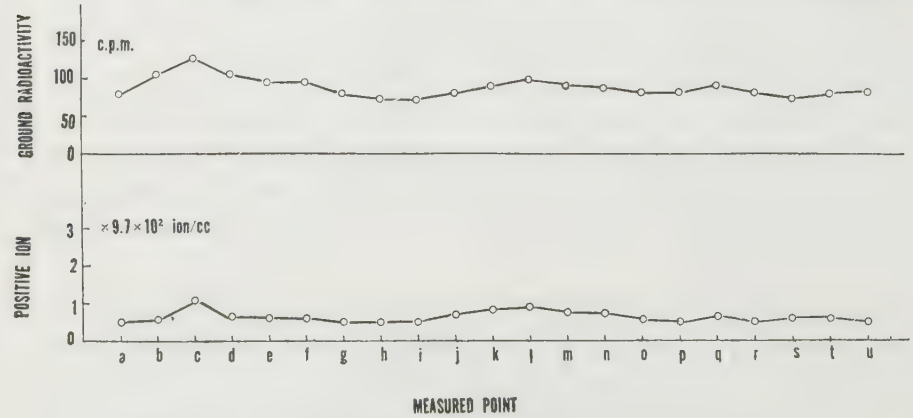


Fig. 26. Ground radioactivity and number of positive ion observed at Hamamura hot spring.

with a clay-bed and gravel. The Radon content of the thermal water is 2～18 Mache, and the ground radioactivity measured by a G-M counter is about 60～85 c.p.m.. This observation was carried out between 11 h and 15 h, when the weather was fine and the wind was blowing from the direction of the lake with a volocity of 1～2 m sec. The correlation coefficient between atmospheric small positive ions and ground radioactivity is calculated as $r=0.62$.

Fig. 28 shows the neighbourhood of the Ikeda mineral spring which is situated

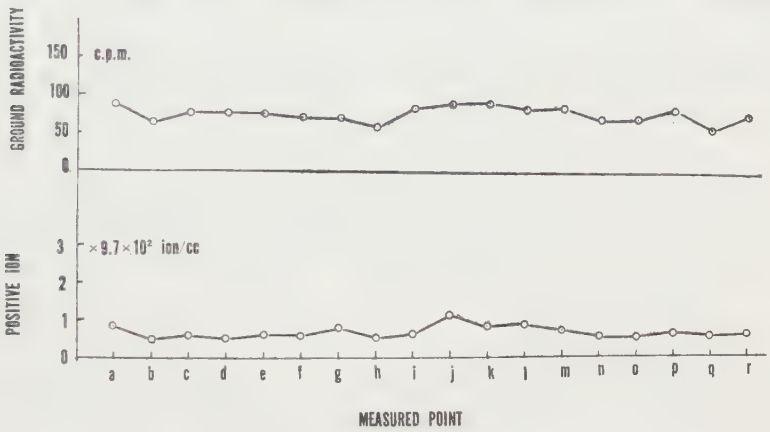


Fig. 27. Ground radioactivity and number of positive ion observed at Togo hot spring.

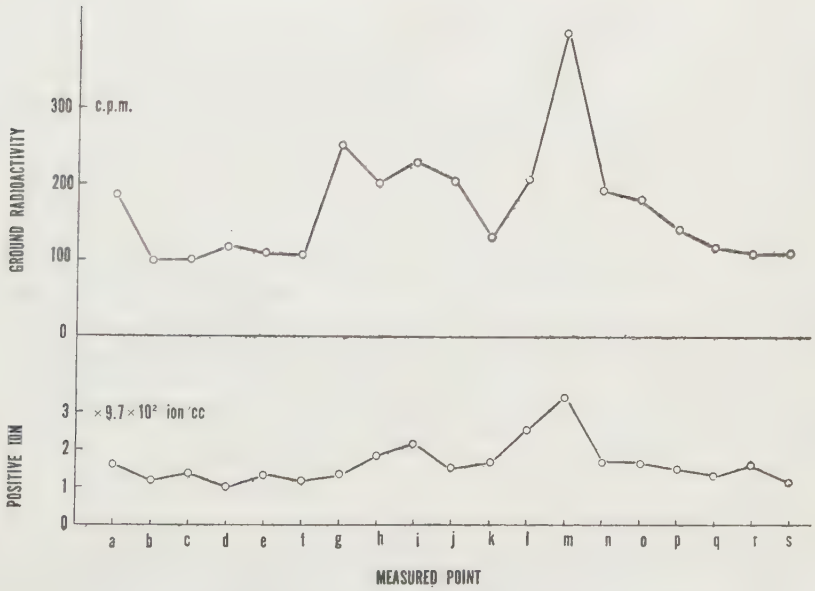


Fig. 28. Ground radioactivity and number of positive ion observed at Ikeda mineral spring.

at the foot of Mt. Sambe. The Radon content of the mineral water is 100～300 Mache and the content of Radium in the mineral water is as strong as $50\times10^{-12}$ g/L.

The ground radioactivity measured by G-M counter shows 100～400 c.p.m.. The measurement was carried out from 9h to 16h when the weather was fine and the wind velocity was almost 1 m/sec. In the observation, some places were covered with a water sheet, and, in spite of a strong ground radioactivity at such places, the counts observed are mainly those of gamma-rays, as no ions would be ionized by alpha-particles and beta-particles at the ground surface by the interruption of the water sheet. For instance, point g was covered with water in the observation, and the correlation coefficient calculated becomes as large as $r=0.90$ if the g-point observation is excluded, and as small as $r=0.83$ when the g-point value is included.

Table 1

| | Correlation coefficient | Ratio of mean ground radioactivity | Ratio of mean ion density |
|---|---|---|---|
| Iwai | 0.50 | 1.00 | 0.56 |
| Misasa | 0.65 | 1.35 | 2.71 |
| Hamamura | 0.52 | 1.10 | 1.06 |
| Togo | 0.65 | 1.00 | 1.00 |
| Ikeda | 0.83 (0.90) | 2.10 | 2.44 |
| mean | 0.62 | | |

Table 1 shows briefly the results of these five observations. The mean value of correlation coefficient is fairly good. As already mentioned in § 3, the rate of atmospheric ionization by cosmic-rays is about 25% and the contribution of atmospheric radioactive substances is estimated to be about 10～20%. Therefore, the contribution of ground radioactivity to the atmospheric ionization may be about 60%.

Moreover, a part of atmospheric radioactive substances is supplied from the ground surface at that point. The rate of contribution of the ground radioactivity will be larger, almost 70%. The effect of the ions moved by the wind may be small, as the mean life of small ions is short. These are the reason why the correlation coefficient of the present subject shows $r=0.62$. And this fact confirms the reports which were already made by the writer on the abnormal value of the electric potential gradient at a spa. (**19**).

## 5. Summary

Recently atmospheric natural radioactivity has been theoretically and practically studied as it has close connection with the atmospheric electricity and other natural phenomena. But the direct measurement of the distribution of atmospheric radio-

activity in the layer of atmosphere close to the ground, and of the relation between atmospheric ions and radioactivity, has not yet been carried out. In the present paper, some practical direct measurements on these phenomena were made, and the following results were obtained:

1) From the direct measurement by nuclear plate camera of distribution of alpha-particles in the air near the ground surface, it was found that the density of alpha-particles in the lower layer of air is small, contrary to the theoretical assumption of Hess. Consequently the application of the theory of eddy diffusion to these phenomena is considered to be inappropriate. The results obtained by the present direct measurement will certainly offer us an important knowledge on the atmospheric ion formation.

2) Measurement of the correlation between atmospheric ion and atmospheric radioactivity has been carried out in the field, and the correlation was ascertained to be conspicuously existing in the night, but not in the daytime. The ratio of atmospheric ions which are ionized by atmospheric radioactive substances to the total ions was calculated to be about 0~80%.

3) From the measurement of the correlation between the earth radiation and atmospheric ions in the field, the mean correlation coefficient was estimated to be 0.62. The percentages of ion formation by earth radiation and by atmospheric radioactivity are presumed to be 60~79% and 10~20% respectively.

**Acknowledgment**

The writer is greatly indebted to the kind guidance and pertinent advice given by Profs. E. Nishimura, K. Kimura and Y. Tamura, of Kyoto University and Dr. M. Kawano (of Elect. Labo.) throughout the present investigation.

REFERENCES

1. E. S. Cotton, J. Atmos. Terrest. Phys., **7** (1955), 90.
2. S. Okabe, Mem. Coll. Sci., Kyoto Univ., A. **28** (1956), 39.
3. S. Okabe, Mem. Coll. Sci., Kyoto Univ., A. **28** (1956), 99.
4. Y. Ito, Bull. Disaster Prev. Res. Inst., Kyoto Univ., **27** (1953).
5. J. Priebsch, Physik. ZS., **16** (1931), 622.
6. V. F. Hess and W. Schmidt, Physik. ZS., **19** (1918), 109.
7. V. F. Hess and G. A. O'Donnel, J. Geophys. Res., **56** (1951), 557.
8. E. Tasima and T. Doke, Kagaku, **26** (1956), 124 (in Japanese).
9. W. Anderson, W. V. May Neord and R. C. Turner, Nature, **174** (1954), 424.
10. M. H. Wilkening, Nucleonics, **10** (1952), 36.
11. C. C. Lauritsen and T. Lauritsen, Rev. Sci. Instr., **8** (1937), 438.
12. G. Ishikawa, M. Kadena and M. Kitamura, Journ. Geomag. Geoelec., **4** (1952), 1.
13. A. R. Hogg, Mem. Comm. Solar Observatory. Cambera, **7** (1939), 1.
14. O. H. Gish, *Terrestrial Magnetism and Electricity*, (New York, 1938), 182.
15. V. F. Hess, Arch. Met. Geophys. Biokl, A. **3** (1950), 56.

16. V. F. Hess and W. D. Parbinson, Trans. AGV, **35** (1954), 869.
17. B. J. Giletti and J. L. Kulp, Am. Mineralogist, **40** (1955), 481.
18. Z. Hatsuda, Mem. Coll. Sci., Kyoto Univ., B. **21** (1954), 231.
19. S. Okabe, Liber. Arts J. Tottori Univ., No. **5** (1954), 10.

MEMOIRS OF THE COLLEGE OF SCIENCE, University of Kyoto, Series A,
Vol. XXVIII, No. 3, Article 4, 1957

# ON THE OBSERVATION OF SECULAR PHENOMENA OF THE TILTING MOTION OF THE GROUND

BY

**Kennosuke HOSOYAMA**

(*Received August 16, 1957*)

ABSTRACT

The observation of crustal deformation at the Kamigamo Geophysical Observatory of Kyoto University, where a highly sensitive tiltmeter is in use, was begun in 1937, and has been continued to the present day. Twenty years of research have thrown some light on questions of importance in geodesy. In the present article I have set out the results of our observation of secular phenomena of the tilting motion of the ground, principally on the basis of the experiments at Kamigamo, but taking into consideration also those conducted at twenty-five other similar stations in Japan. In such work as this, problems arise concerning the reliability of the instruments employed, the solidity of the foundations in which the instruments are set, the disturbing effects of meteorological change, local conditions as they affect the place of observation, and similar matters: I go into those questions in some detail. The conclusion reached in this paper is, that the observation of secular phenomena carried out by means of tiltmeters of a high degree of sensitivity at a sufficient number of places in a limited area are probably to be considered as being of value in detecting the phenomena that preceed destructive earthquakes, provided, of course, that the observations are carefully made and correctly interpreted. Knowledge of such precursory phenomena is of value in determining the nature and mechanism of earthquakes.

## 1. Introduction

There are two methods used for studying crustal deformation; the one is to trace the process of past crustal deformation in geologically long times by observing the topography, geological structure and some phenomena concerned with them, and the other is to investigate the progressing crustal deformation by means of geodetic methods. The results that are obtained by the former investigation are the integrated deformation with the career of geological ages, and they can, in general, hardly be connected with and applied to the investigation of the nature of the present crustal deformation now in progress. For this purpose the latter method of geodetic measurement has been profitably used. It should be mentioned here that the term "crustal deformation" properly means the upheaval, subsidence, and horizontal displacement of the ground with reference to the mean sea-level or any point assumed to be unchangeable. But recently, it is also used in a more widely extended meaning to describe the phenomena of secular variation in gravity-intensity, plumb-line deviation, geomagnet-

ism, and other geophysical elements which are considered to be caused by or related to the activity or the change of state in the constituent material of the earth's crust. Especially, the crustal deformation, in a wider sense, with relation to the occurrence of destructive earthquake, or the great eruption of volcanoes, has ever been an attractive and important research item in seismology and geodesy.

Investigation of crustal deformation in Japan by level surveying and triangulation was commenced shortly after the Nobi Earthquake in 1891. These survey methods were suitable and productive in studying the relation between earthquake-occurrence and ground-deformation. At present, in our country, the area surveyed has increased yearly, especially in some districts disturbed by great earthquakes where repeated surveying has resulted in important findings (**1**, **2**, **3**, **18**, **19**, **20**). However, as it is difficult, mainly for financial reasons, to carry out this sort of levelling survey and triangulation extensively in a region with frequent repetition, observations with some geodetic instruments of automatic and continuous recording at many fixed stations have gained prevalence, supplementing level- and triangulation-surveys.

In the present article, the observations, especislly those of secular phenomena, of the tilting motion of the ground caused by crustal deformation, made with a highly sensitive tiltmeter and at many different stations in our country are here reported and discussed in some detail. As the silica-tiltmeter of a horizontal pendulum type devised by M. Ishimoto (**4**, **5**) is highly sensitive and easily manipulated, the instrument has been frequently employed, in our country, in the study of earth-tides and, also in the study of the tilting motion of the ground, as a station instrument. In the research field of instrumental-observation of ground-tilting which is supposedly connected with the earthquake-occurrence, many papers have been published since Ishimoto's in 1929 (**4**), by M. Ishimoto (**4**, **5**), U. Inoue and T. Sugiyama (**6**), K. Sassa and E. Nishimura (**7**, **21**), K. Hosoyama (**14**, **16**), E. Nishimura and K. Hosoyama (**15**), T. Hagiwara (**8**), and others. Observations were made mainly with the silica-tiltmeter of the Ishimoto-type, the invar-tiltmeter of the Nishimura-type and others. Hagiwara has suggested that the water-tube tiltmeter which measures the difference between the water level at two points at a great distance apart is more suitable than the tiltmeter of horizontal-pendulum type in the investigation of secular ground-tilting. The relative merits of the instruments of these two types really should be judged from the standpoint of object in phenomena. For the purpose of investigating the minute tilting-motion of the ground as caused by the earth-tides, forerunning phenomena of short duration just before the earthquake-occurrence, and other micro-geophysical changes, the highly sensitive tiltmeter of horizontal-pendulum type is more profitably used. On the contrary, the water-tube tiltmeter is suitable, in general, for the observation

of slow ground-tilting of an extended period of several years. Generally, in the observation of secular tilting motion of the ground, the following conditions should carefully be considered. These arguments are applicable to both cases of observation with the water-tube tiltmeter and the horizontal pendulum tiltmeter, but, in the present article, those with the latter are mainly discussed. The principal effects which are considered to disturb the observational results are; (1) degree of instrumental stability, (2) meteorological effect, (3) local character of observation-place and room, and other troublesome effects.

Concerning the degree of instrumental stability, some experimental observations comparing the results of the horizontal pendulum tiltmeter with those of other types were made, and it was ascertained that the tiltmeter with a horizontal pendulum can advantageously be utilized for the study of the secular tilting motion of the ground, when some appropriate precautions are taken against the manipulation of the instrument, the selection of the observation position, etc.

Secondly, on meteorological effects, namely those by daily and annual variation of atmospheric and ground temperature, and, moreover, by rainfall and sunshine have been treated by some researchers (**9**, **10**, **11**, **12**, **13**). It is contended however that a general law on the disturbing effect of meteorological change upon the observed result of ground-tilting cannot so easily be found, as the meteorological change has considerably strong local characteristics in each case of observation. The problem concerning meteorological effects can certainly be solved by the inbedding of the instrument in the observation room, say 100 m or so below the ground surface as any meteorological effect is ostensibly eliminated.

Thirdly, the problem on local character of the observation place is most difficult and essential in this sort of observation. Here, the meaning of "local character" should be examined and classified. It is, in the present paper, used to denote the particular tilting motion of the foundation on which the tiltmeter is set up, the observation room, the observation station, and the obrervation area within a radius of several kilometers.

These three disturbing effects should carefully and fittingly be reduced and corrected in precise observations on tilting motion of the ground, especially on those connected with the earthquake-occurrence. Regarding these points some detailed discussion will be made in the following. In consequence the observed data for the extended 20 years period from 1937 till 1957 at the Kamigamo Geophysical Observatory will first be discussed in reference to the disturbing effects, and afterwards the arguments will be extended to other stations. Finally the trustworthiness of some previously obtained data on peculiar tilting motion of the ground which are supposed to be intimately connected with and to forerun earthquake-occurrence, will be examined and

discussed from various aspects. For the sake of facilitating comprehension, the positions of main observation stations will be shown in Fig. 1.

Fig. 1. Position of observation stations.

## 2. Secular tilting motion of the ground observed at the Kamigamo Geophysical Observatory

The Kamigamo Geophysical Observatory of Kyoto University is located on a mountain top about 100 meters high, in the northern part of Kyoto City. The mountain rock is of the paleozoic system. The instrument is silica-tiltmeter of horizontal pendulum type, and the observation room is in a pit, 9 meters deep under the ground surface.

Mean sensitivity of the tiltmeter has been maintained at about 0″.005/mm, and the positive direction of the A-component indicates the tilting motion of the ground downwards to N45°E and the B-component to S45°E. The observation was commenced early in 1937 and has been continued to the present, encompassing a long series of observations. Fig. 2 shows the monthly mean of ground-tilting during 17 years of the 20 years and each component clearly shows the annual variation. Some researchers have discussed the causes of such annual variation, and have concluded that it is caused by seasonal effects such as change of atmospheric temperature, baro-

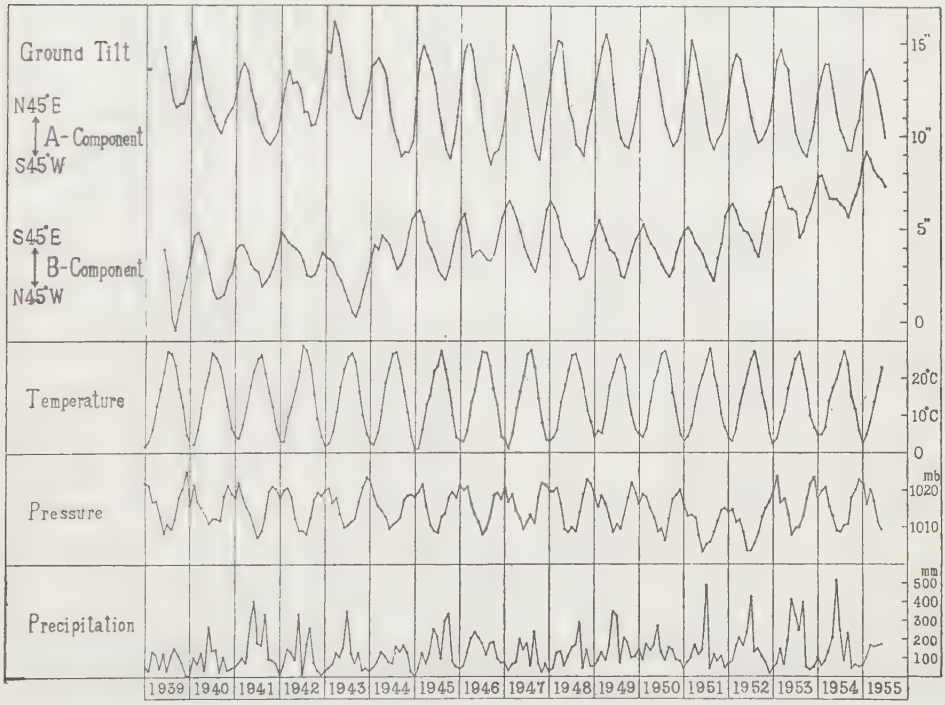


Fig. 2. Annual variation of ground-tilting observed at Kamigamo.

metric pressure, and other meteorological variations. Really, also in the present case, there exists, in general, a great similarity among these changes, as seen in Fig. 2.

But, examing these relations in detail, the following two points peculiar to ground-tilting are easily detected. Namely, the large fluctuation of amplitnde in annual variation and the secular change of the annually mean value with regard to ground-tilting are characteristic, compared with the regular annual variation of atmospheric temperature and pressure, as shown in Fig. 2. More fully discussed, a vector diagram of ground-tilting for each year is described in Fig. 3, and the form of annual variation is roughly said to be similar to the other. The direction of maximum axis in the

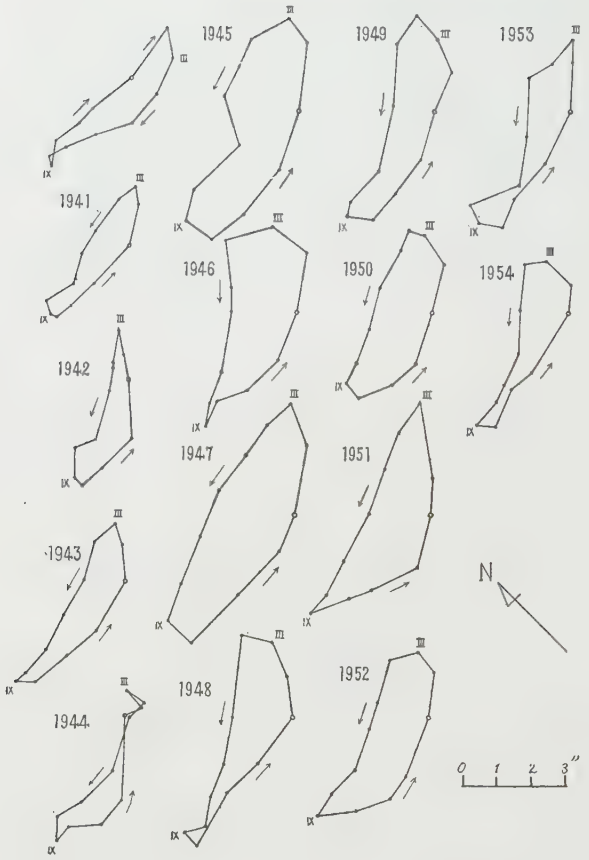


Fig. 3 Vector diagram of annual ground-tilting observed at Kamigamo.

variation being nearly E–W. March and September have the highest variation values. But, in delailed treatment, the fluctuation of amplitude in annual variation, expressed in the yearly change of length of long and short axes in the vector diagram, is clearly observed, and they are ascertained to be intimately connected, as shown in Fig. 4, to yearly change of mean atmospheric temperature. And, as also noted in the figure, the rate of secular variation, as calculated from the residual ground-tilting under the assumption of perfect closure in the vector diagram of annual variation, is somewhat correlated to the yearly total value of rainfall. These correlations between the ground-tilting and meteorological changes are considerably complex in their correspondence and have excessively localized character as seen in each observation at different places. But it is important to get a clear knowledge about these correlations in every case of observation, for the sake of precise and accurate investigation with respect to ground-tilting; whereof, detailed discussion will be made in a later section. Here, for

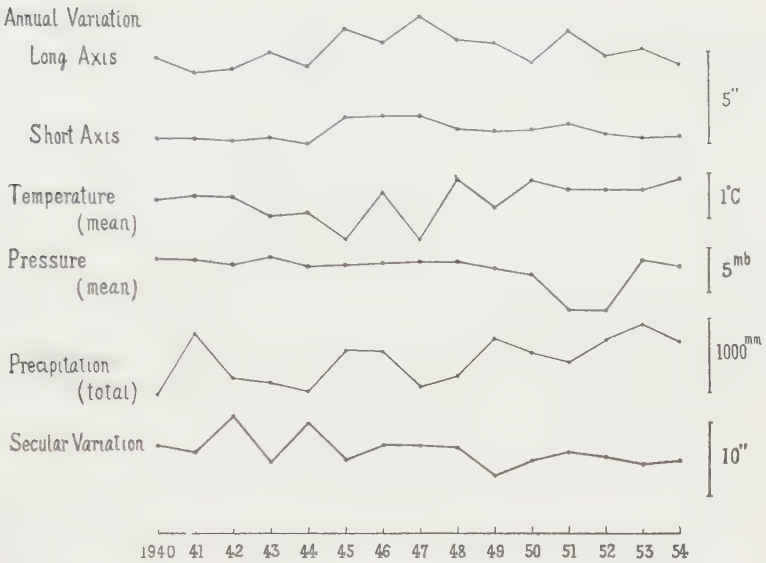


Fig. 4. Elements of secular ground-tilting observed at Kamigamo.

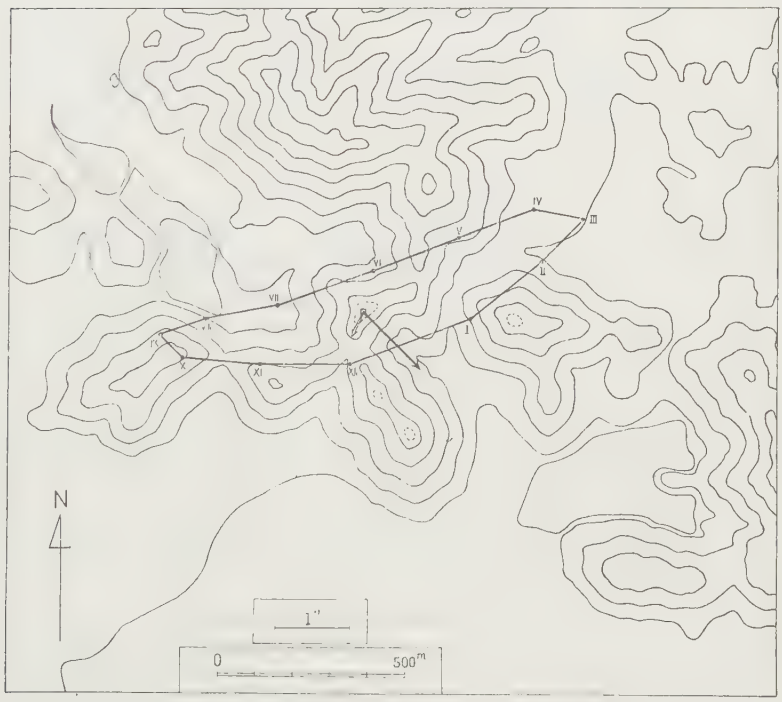


Fig. 5. Modes of annual ground-tilting, secular variation, and rainfall effect at Kamigamo.
closed vector-diagram : annual variation
➡ : secular variation ⇨ : rainfall tilting

the sake of reference, the graph of topography with vector diagrams of mean annual variation, and secular variation of ground-tilting, and, moreover, the direction of ground-tilting, in the case of rainfall at Kamigamo, are schematically shown in Fig. 5. It is questionable as to whether or not there is any significance in the relative directions of ground-tilting caused by its respective changes. Next, with regard to the secular behaviour of ground-tilting as described in the vector diagram, Fig. 6 will be subsequently referred to, the diagram being obtained from the values of the running mean of each 12 months during the 1939–1955 period. From the figure it is seen that the ground has tilted downward to S in the first stage of 1939–1942, then reversely to N in the 1942–1943 stage; again to S in 1943–1945, and, after the slightly oscillating motion, has steadied itself toward S–E, from 1951 until the present. The total amount of ground-tilting at Kamigamo is estimated to be nearly 5″ during the past 17 years.

Finally, concerning the relations between secular tilting motion of the ground observed at Kamigamo, and the occurrence of earthquakes in the neighbouring districts, the secular variations observed by each component tiltmeter (A and B) are separately plotted in Fig. 7 for the convenience of easy understanding with the occurrence of large earthquakes which occurred in the neighbouring area of Kamigamo. The name of earthquakes whose occurrence times are indicated by arrows in the figure are (1) Tottori (Sept. 10, 1943), (2) Tonankai (Dec. 7, 1944), (3) Mikawa (Jan. 13, 1945), (4) Nankaido (Dec. 21, 1946), (5) Fukui (June 28, 1948), (6) Daishoji-oki (Mar. 7, 1952), (7) Yoshino (July 18, 1952).

As great earthquake close by Kamigamo has not occurred during the observation-period, the correlation between the secular variation of ground-tilting and the occurrence of large nearby earthquakes was not definitely ascertained. But if it is examined in detail with the anticipation of finding a correlation some correspondence between will be found, especially conspicuous in case of the Tottori Earthquake of 1943, less markedly in the instance of the Tonankai Earthquake of 1944, the Nankaido Earthquake of 1946, the Fukui Earthquake of 1948, and the Yoshino Earthquake of 1952. In all these examples a particular tilting motion which might be said to be a ground-tilting forecasting the earthquake-occurrence, was observed to have appeared during the period of nearly one year before the earthquake-occurrence. But, as this sort of discussion may contain many difficult and questionable points, a detailed treatment will be postponed to § 6.

Much of the foregoing discussion referring to the data obtained by the long period of observation nearly 20 years at the Kamigamo Geophysical Observatory will undoubtedly be supported and advanced by the numerous data observed at other observation stations which are more than 25 attached to Kyoto University and which are advantageously distributed in a dense net throughout Japan. In the next section the observed data at these stations are treated.

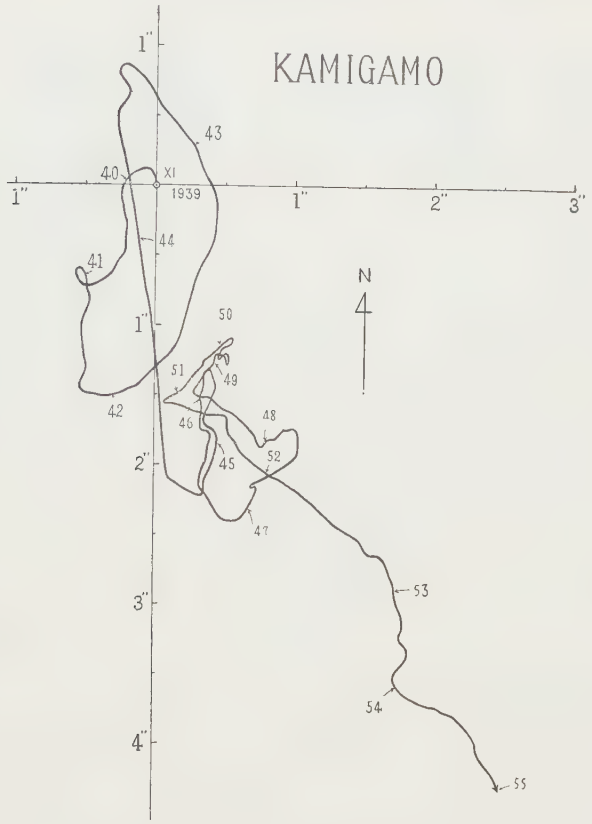


Fig. 6. Vector-diagram of secular ground-tilting observed at Kamigamo.

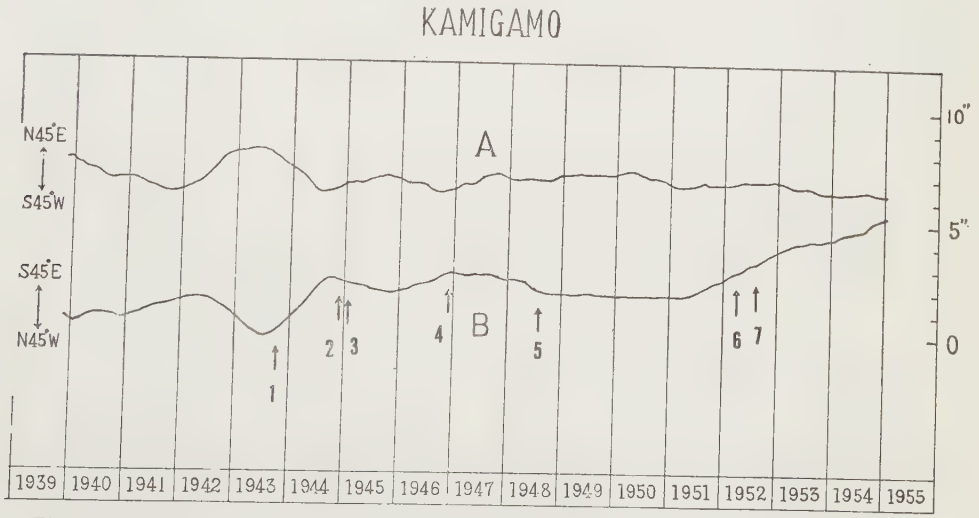


Fig. 7. Relation between the secular ground-tilting expressed in two orthogonal components and the neighbouring destructive earthquakes observed at Kamigamo.

Table 1

| Station | | Position E | Position N | Height on sea level | Geological formation of ground rock | Underground depth of observation room | Type of tiltmeter (horizontal pendulum) | Epoch of observation |
|---|---|---|---|---|---|---|---|---|
| Makimine | 1 | 131°27′ | 32°37′ | 130 m | Paleozoic | 165 m | Silica (1942–47) Superinvar (1948–) | 1942– the present time |
| | 2 | ″ | ″ | ″ | ″ | 165 | Superinvar | 1952– the present time |
| Beppu | 1 | 131 30 | 33 16 | 10 | Alluvial sand and volcanic lava | 2 | Silica | 1937–38 |
| | 2 | ″ | ″ | 20 | ″ | 3 | ″ | 1937–39 |
| | 3 | ″ | ″ | 30 | ″ | 2 | ″ | 1937–39 |
| | 4 | ″ | ″ | 150 | ″ | 5 | ″ | 1938–39 |
| Kōchi | | 133 32 | 33 34 | 10 | Paleozoic | 40 | Superinvar | 1949– the present time |
| Bessi | | 133 19 | 33 52 | 660 | Chlorite-schist | 750 | ″ | 1949–51 |
| Shionomisaki | | 135 47 | 33 28 | 8 | Porphyrite | 5 | ″ | 1955– the present time |
| Kishu | | 135 53 | 33 52 | 90 | Tertiary sandstone and shale | 60 | ″ | 1957– the present time |
| Susami | | 135 30 | 33 32 | 5 | Paleogene | 10 | ″ | 1948– the present time |
| Yura | | 135 07 | 33 57 | 10 | Mesozoic sandstone and shale | 30 | ″ | 1951– the present time |
| Tamamizu | | 135 49 | 34 48 | 250 | Paleozoic | 30 | ″ | 1948–51 |
| Kamigamo | | 135 46 | 35 04 | 190 | Paleozoic | 9 | Silica | 1937– the present time |
| Ikuno | 1 | 134 50 | 35 10 | 440 | Liparite | 237 | Superinvar | 1951– the present time |
| | 2 | ″ | ″ | ″ | ″ | 326 | ″ | 1952–53 |
| | 3 | ″ | ″ | ″ | ″ | 719 | ″ | 1943–53 |
| Nakahama | | 133 15 | 35 30 | 10 | Alluvial sand | 2 | Silica | 1938–40 |
| Ogaya | | 136 33 | 36 17 | 210 | Tertiary tuff | 300 | Superinvar | 1948– the present time |
| Kamioka | | 137 19 | 36 21 | 920 | Gneiss | 800 | ″ | 1952– the present time |
| Hosokura | | 140 54 | 38 48 | 130 | Tertiary | 160 | ″ | 1944– the present time |
| Tottori | | 134 17 | 35 31 | 150 | Liparite | 200 | ″ | 1955– the present time |
| Aso | 1 | 131 00 | 32 53 | 540 | Volcanic rock | 22 | Silica | 1937–40 |
| | 2 | 131 03 | 32 53 | 1130 | ″ | 10 | ″ | 1937–40 |
| | 3 | 131 07 | 32 57 | 520 | Volcanic ash | 3 | ″ | 1937–40 |
| | 4 | 131 05 | 32 53 | 1150 | Volcanic lava | 1 | Silica (1937–43) Superinvar (1953–) | 1937–43 1953– the present time |
| Iimori | | 135 26 | 34 15 | 220 | Chlorite-schist | 40 | Superinvar | 1943–45 |
| Ide | | 135 49 | 34 48 | 150 | Paleozoic | 15 | ″ | 1951– the present time |
| Abuyama | | 135 34 | 34 52 | 200 | Paleozoic | 20 | ″ | 1938– the present time |
| Osakayama | | 135 51 | 34 59 | 130 | Paleozoic | 150 | ″ | 1947 the present time |
| Tsuchikura | | 136 18 | 35 36 | 400 | Paleozoic | 170 | ″ | 1953 the present time |
| Osarizawa | | 140 45 | 40 11 | 320 | Tertiary tuff and shale | 300 | Silica | 1944 46 |
| Suhara | | 135 12 | 34 03 | 5 | Chlorite-schist and breccia | 60 | Superinvar | 1955– the present time |

### 3. Secular ground-tilting observed at various observation stations

The total number of our stations for observing the crustal deformation is nearly 33 during the past 20 years. Some of them were temporary stations during the first few years for studying special items, but the majority of them were permanent stations which have been increased each year, the number of the permanent stations being 19. We intend to increase the number of stations, all being equipped with a tiltmeter, an extensometer, a gravity-variometer, a magnetic variometer, and other instruments, to 25 permanent stations during the international geophysical year of 1957–1958. In Table 1, the details of each observation station are described, including the temporary, the permanent stations, and the scheduled stations.

In the following sections, the data obtained at various stations where the geological conditions, the depth of the observation room, the topography and other circumstances differ widely from each other, will be analysed and discussed as regards the type of instrument, the instrument-foundation, the meteorological effect, and the local character of the ground-tilting. In Figs. 8a–8n, some examples of the mode of

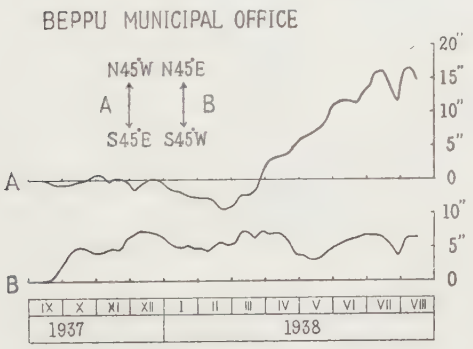


Fig. 8a.

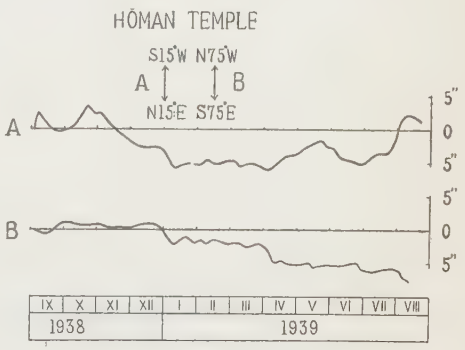


Fig. 8b.

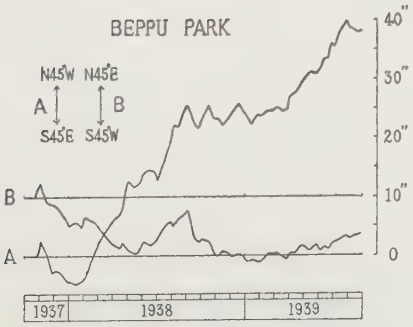


Fig. 8c.

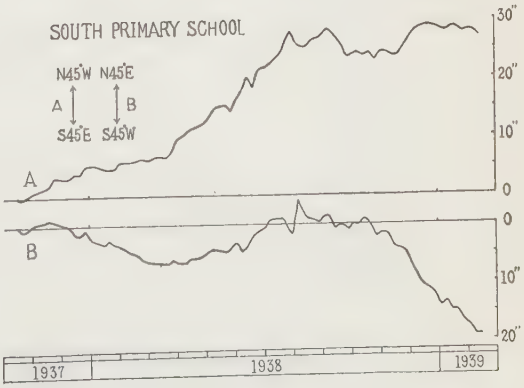


Fig. 8d.

secular ground-tilting observed at various stations are shown. As seen in these figures, the mode of ground-tilting differs widely for each station, namely, one shows a periodic motion like an annual variation, and the other a chronic motion toward a certain direction. The former is generally observed at stations with a shallow seated observation room, shallower than about 10 m, and the latter is often observed at stations with a deeply seated observation room, more than several hundred meters deep, which is usually a part of an adit in a metal mine. From these facts, it can simply be explained that an observation in a shallow room is largely affected by meteorological changes, such as daily and seasonal changes of air-temperature and ground-temperature, and the amount of precipitation. The observation in a deep room is usually disturbed by a gradual but progressive deformation of an adit by the rock pressure more than one-thousand atmospheric pressure and its change caused by mining at the neighbouring adit. Really, it is observationally ascertained that the progressive tilting motion to

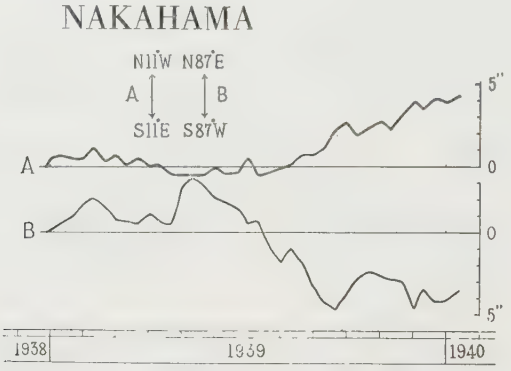


Fig. 8e.

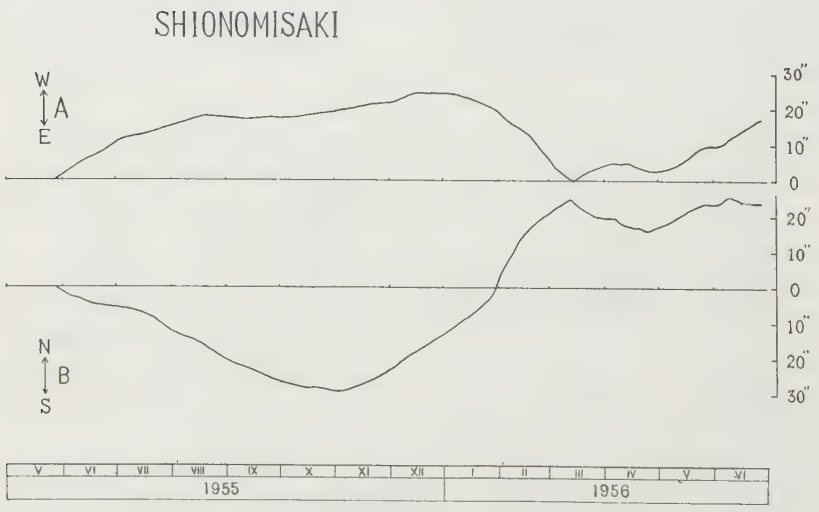


Fig. 8f.

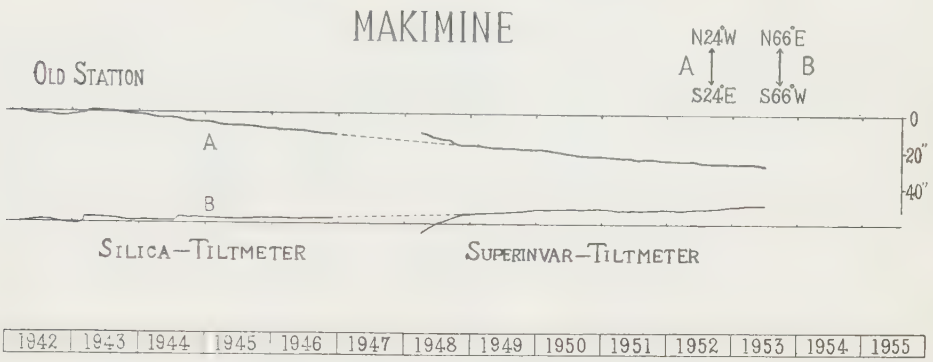


Fig. 8g.

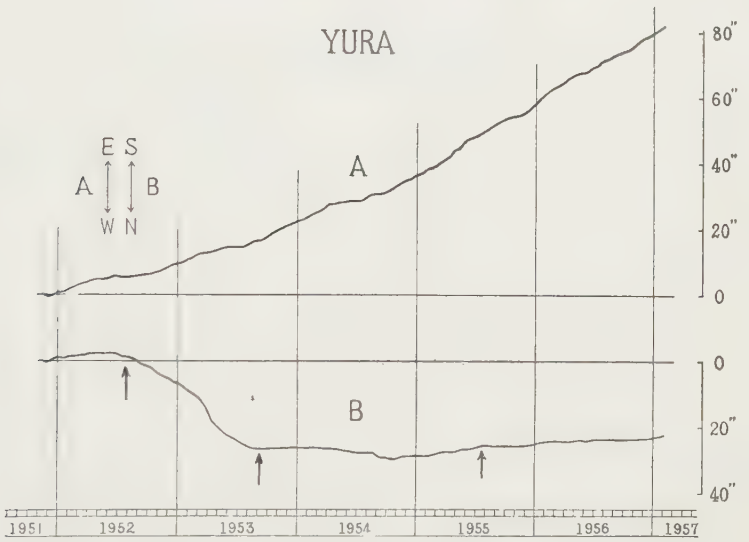


Fig. 8h.
Arrow indicates the time of occurrence of neighbouring large earthquakes.

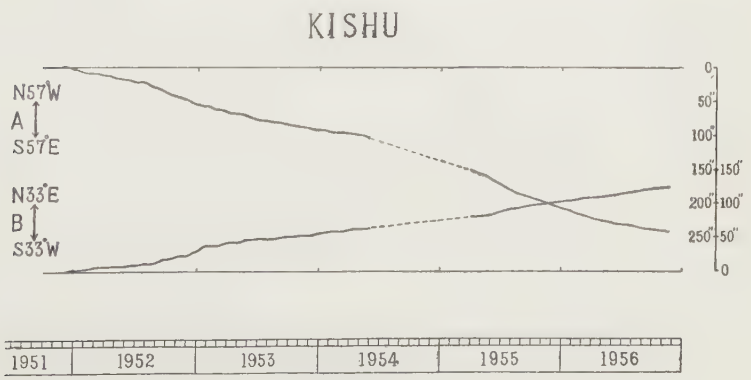


Fig. 8i.

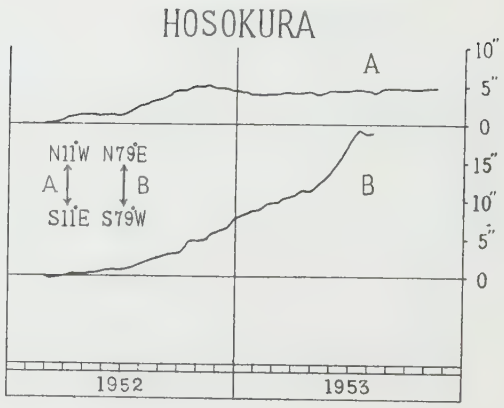


Fig. 8j.

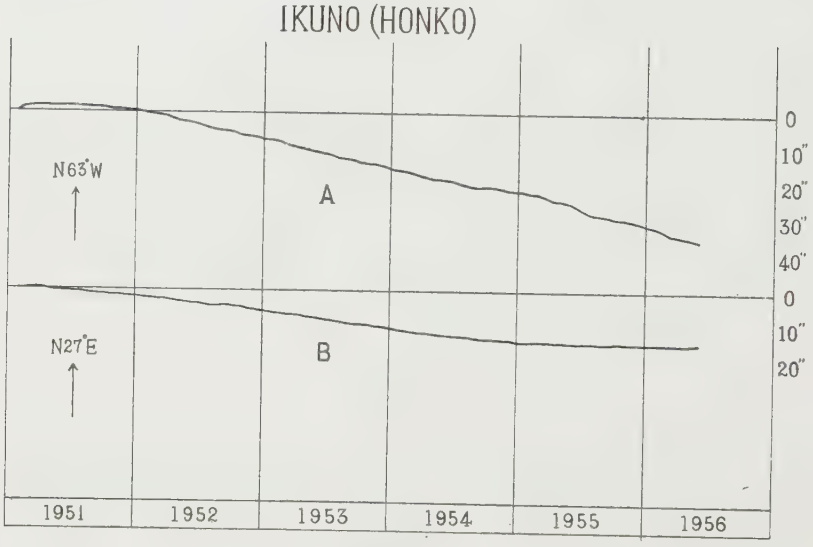


Fig. 8k.

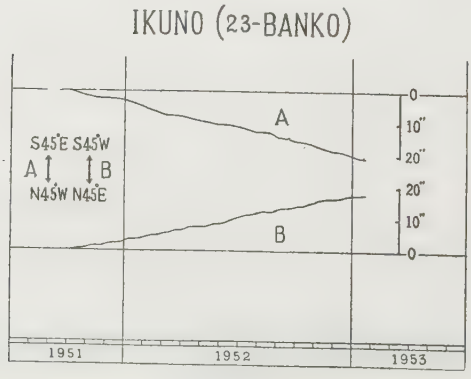


Fig. 8l.

one direction observed at a shallow seated room is, in the usual case, exceedingly small, in spite of a large daily and seasonal variation of ground-tilting, and rainfall-influence. On the contrary, however, observation in a deep seated room is little affected by meteorological change and seasonal variation. Some details on the relative merit of the underground depth of an observation room will be referred to in a later section.

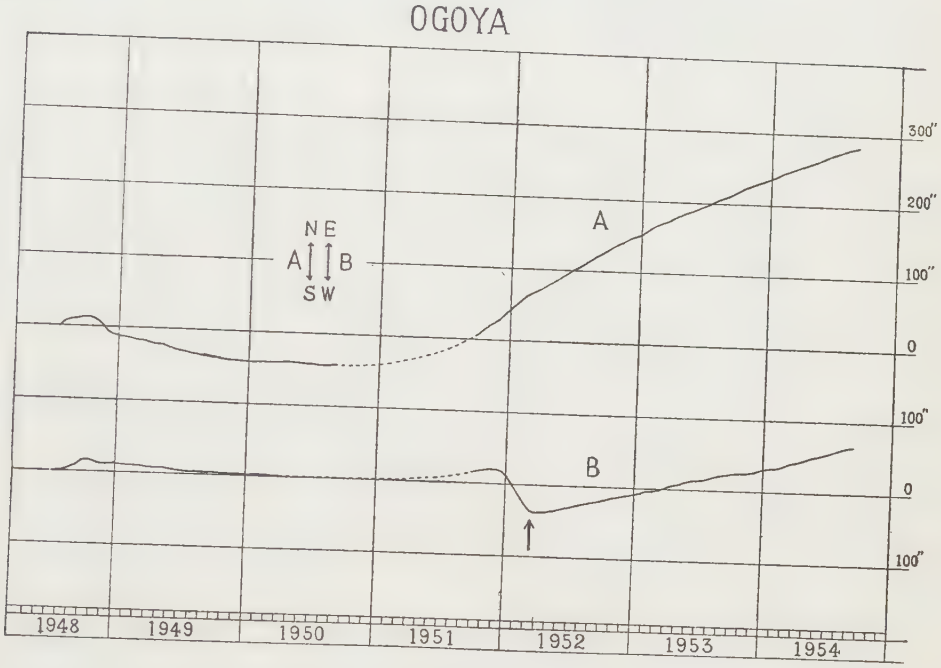


Fig. 8m.
Arrow indicates the time of occurrence of Daishoji-oki Earthquake.

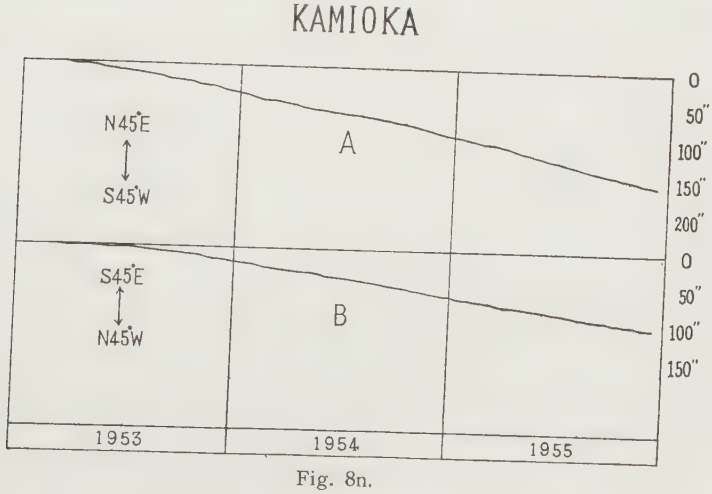


Fig. 8n.

### 3. Effects of various causes upon the secular observation of ground-tilting

It has already been remarked in the previous section that the secular observation for tilting motion of the ground is generally disturbed by various causes. For the sake of precise study on the nature and mode of real ground-tilting, these disturbing causes must be carefully examined and completely removed. Some detailed treatments are made in the present section concerning these causes.

*(1) Type of tiltmeter*

As the principal parts of a silica-tiltmeter with a horizontal pendulum are made of fused silica, the direct temperature effect upon the pendulum is very small. The tiltmeter of this type shows good stability in a long series of observations, and really the original silica-tiltmeters set up early in 1937 at Kamigamo have been operated until the present time without interruption. But the making of a tiltmeter of this type needs special skill, consequently, when it is damaged, it is practically impossible to repair it when being used in the field. Moreover, micro-oscillations are frequently observed in the tiltgram of the silica-tiltmeter even when the tiltmeter is set in a deep seated room. The sources of these micro-oscillations have not yet been definitely identified, but they are supposed to have mainly originated from the micro-oscillation of the silica-pendulum moved by the minute circulation of air in the circular cylinder, covering the pendulum parts, which is, of course, air-tight. This disturbance is considered to be mainly attributable to the point of light weight of inertia mass, weighing only 1 gram, in a horizontal pendulum.

E. Nishimura constructed the superinvar-tiltmeter of horizontal pendulum type to remove these inefficiencies in the silica-tiltmeter. To put it more precisely, the main parts of the tiltmeter, the horizontal pendulum and its supporting-frame, are made of superinvar alloy, the weight of inertia mass, the radius of suspension superinvar wire, the length of pendulum-arm and the height of supporting-frame being 15 grams, 15$\mu$, 10 cm and 20 cm respectively. However, only for the material of inertia mass pure electric copper plated with gold is especially used to preclude any magnetic effect. By means of these improvements the micro-oscillation as frequently observed in those cases of obser vation in which the silica-tiltmeter is used, is greatly reduced in frequency and amplitude. Concerning the function-comparison between the silica- and superinvar-tiltmeters, some test observations were made at several stations in a comparatively short period of several months. Of these results obtained by short period observation, both tiltmeters were ascertained to show the same results, with regard to both periodic earth-tidal change and secular ground-tilting. As an example of the long-period comparison observation between the silica and- superinvar-tiltmeters, Fig. 8g is conveniently referred to, where the secular ground-tilting observed at Makimine is

plotted. Though it is regrettable that there is no simultaneous observation using two tiltmeters, it is clearly shown in Fig. 8g that observations both with the silica-tiltmeter (1942–1946) and the superinvar-tiltmeter (1949–1953) have similar ground-tilting toward common direction, excepting the abnormal change in the initial epoch just after the commencement of the observation in both cases. Fig. 9 indicates the comparison between two superinvar-tiltmeters of the same type made at the Abuyama Seismological Observatory, Kyoto University, during the period from January to April 1951. In this case the comparison was made by one component, and both tiltmeters have been

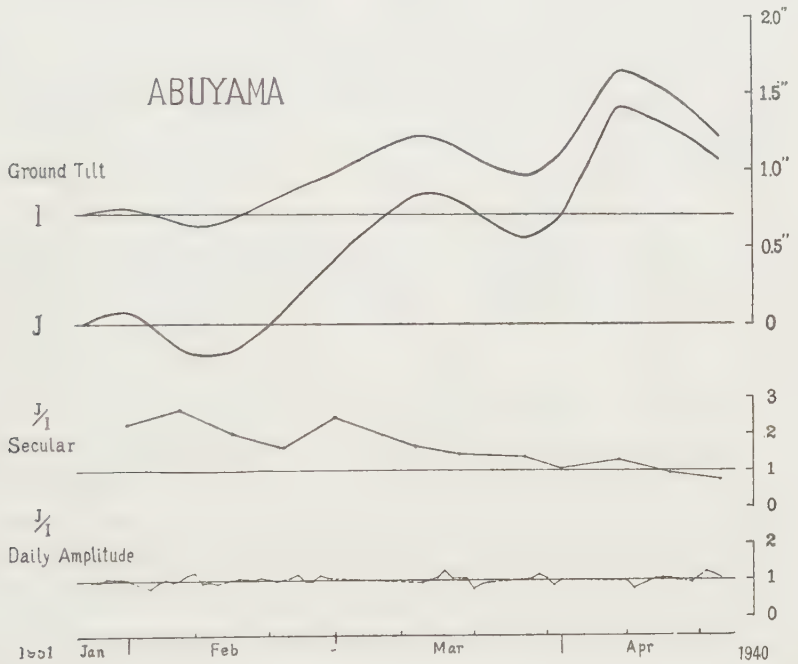


Fig. 9. Comparison observation with two superinvar tiltmeters at Abuyama.

set in the same direction with similar sensitivity of 0″.116/mm. As seen in Fig. 9, both tilting motions show a similar tendency, but their secular variation quantities seem to be somewhat different. The ratio of amount of tilting-motion J/I is about 2 at the initial stage, but becomes gradually nearly unity. From these and other cases it is losely concluded that the secular ground-tilting is, in general, disturbed during the initial stage, just after the setting up of the instrument. However, it gradually reaches a normal state after a few months, at most, from the initial observation. But it should be emphatically remarked that the ground-tilting of short period, such as earth-tidal change or daily-variation and others, is observed, in perfect similarity of form and amplitude, with two tiltmeters of the same type or of different type.

As an example of the former case of the same type, the ratio of amplitde of daily gronnd-tilting observed at Abuyama is plotted every day. This means that the short period ground-tilting is little affected by the disturbing effect of setting up the instrument. And as in the latter case of a different type the result of a comparative observation between the superinvar-tiltmeter and the mercury-tiltmeter during 7 months at Yura was in some detail reported by the writer (**16**). Here, the disturbing effect of the initial setting up of the instrument for the secular ground-tilting and the perfect coincidence of two tiltmeters with respect of the short period ground-tilting, are both clearly ascertained as was done at Abuyama.

Generally speaking, the disturbing effect of instrumental error upon observations over a longer period, that is, a period of several years, has not yet been examined. While the task of making comparison observations over a period of say 50 or 100 years, using several tiltmeters of the same type or of different types at some suitable observation rooms would be an operose one, it is at the same time a most essential which should be undertaken for the furtherever of accurate knowledge of the nature of secular ground-tilting. However, under the present circumstances, the following method for verifying the authenticity of observed secular change is readily, though tentatively, used in practical cases. One tiltmeter set of a horizontal pendulum type is constituted of two pendulums orthogonally arranged to each another, that is A– and B–pendulums. When the ground tilts in the direction of the B–pendulum, it is enlargedly recorded by A–pendulum, by slightly disturbing the degree of horizontality of B–pendulum, in other words, changing the free period of B–pendulum slightly. Although these changes in pendulum-period are usually minute, but in case of the accumulation of secular ground-tilting during several years, they reach measurable amount. And in practical cases, this simple method has been occasionally and advantageously used to examine the reality of secular change of ground-tilting. In almost all cases, the secular changes observed are ascertained to be the real ground-tilting itself, and not those apparently observed by instrumental and other errors.

(*2*) *On instrument-foundation*

Several kinds of foundation on which the tiltmeter is set have been used in our present observations. These are natural rock, granite foundation artificially shaped, and concrete foundation, discriminatingly used according to the circumstances and conditions of the observation room. If the instrument could be set on natural rock, it is the most desirable observationally, but as such favourabe conditions are seldom obtainable, the artificial foundations are generally used. The granite-foundation, artificially shaped (usually in the size of $50\times100\times10$ cm), is also suitable for secular observation of ground-tilting when a certain care is taken to establish a firm connec-

tion between the granite-foundation and the base rock. But, under some circumstances, a reinforced concrete-foundation, usually in the size of $100 \times 150 \times 30$ cm, is used for the ordinary observation. Whenever the concrete foundation is utilized the disturbing effects caused by the deformation of the foundation during the process of the concrete solidifying and the creeping phenomenon of the foundation by the heavy instrument, and other unknown origins should be carefully examined. Generally, where a concrete-foundation is employed it is not used for nearly 6 months after concretion, and moreover the data observed during the initial period of about 6 months are adopted only as a reference in the study of secular ground-tilting. For example, the data observed at Makimine is referred to in Fig. 8g. The superinvar-tiltmeter was set up in 1948 on the same concrete foundation which has been used for a silica-tiltmeter from 1942 to 1946. As shown in Fig. 8a, the ground-tilting has the same tendency in both cases excepting half a year's abnormal change observed in the early period of observation. Consequently, the concrete-foundation can satisfactorily be used when some care is taken in securing a firm connection between the foundation and base rock, prevention of the deformation caused by concrete-solidification, and the creep phenomenon, and moreover, certain attention is paid to the treatment of data gained in the initial stage after setting up the instrument.

A test observation on the nature of concrete- and granite-foundation was made at Ikuno. Namely, two superinvar-tiltmeters of the same type were set on two different foundations, one of concrete and the other of granite of nearly the same size, which are placed 2 m apart in the same adit, and several month's observation for comparison was carried out. The result was that the secular ground-tilting observed was sufficiently similar for both tiltmeters, excepting in the initial month's data. From this it is generally concluded that any sort of foundation will sufficiently serviceable for tiltmetric observation of secular ground-tilting when specific attention is paid to the elimination of undesirable, disturbing effects.

*(3) Meteorological effect*

The effects of meteorological changes upon the ground-tilting have been discussed by some researchers. These effects are exceedingly large in amplitude and are extremely complicated in character when observation was conducted on the ground surface or in a shallow seated room. On the temperature change of air and soil or rock, their effects directly upon the parts of the instrument were ascertained to be negligible by some test experiments. Especially since the parts of horizontal pendulum and its supporter are made of fused silica (its linear expansion coefficient being $4 \times 10^{-7}$) or superivar alloy (its linear expansion coefficient being $3 \times 10^{-7}$), the temperature effect upon the instrument itself is neglected in ordinary instances. But especially the effect of the daily and seasonal changes of temperature upon ground-tilting is generally

much greater (several scores of times) in amplitude compared with earth tidal ground-tilting in an observation in a shallow seated room. From observations of ground-tilting by a superinvar-tiltmeter at an ordinary underground room of 2 meters depth below the ground surface, recording at the same time the air temperatures both outside and inside the observation room, it was ascertained that the daily variation of ground-tilting was observed in accordance with the change of the outdoor temperature, not so much with the change of room temperature the phase of which is 2 hours behind that of outdoor temperature. From these and other sorts of experimental observation the so-called daily and seasonal variations of ground-tilting are interpreted as mainly attributable to the buckling deformation of the building and ground in which the observation room is situated. Air and soil (or rock) temperature changes cause this buckling deformation in a complex manner under various conditions with regard to the surrounding topography of the observation station, the amount of solar radiation, the geological formation, and many other conditions.

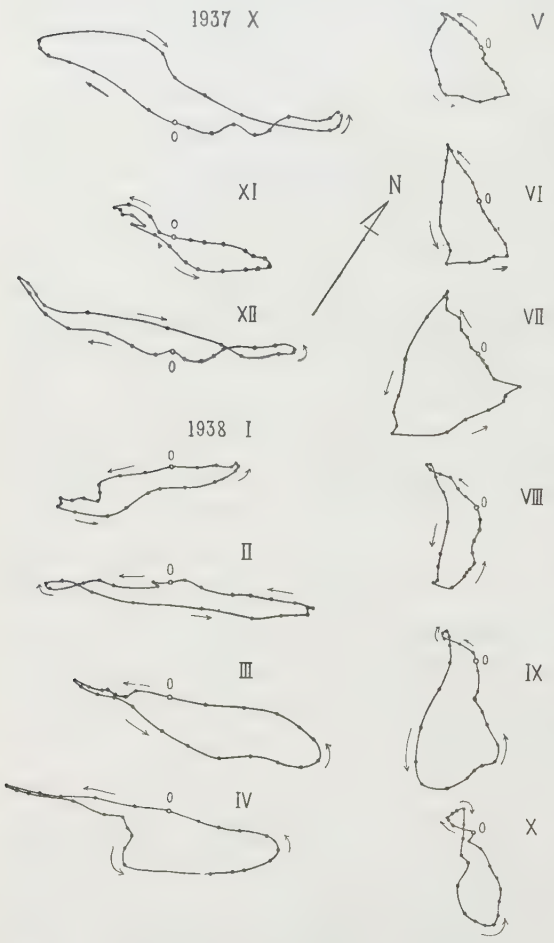


Fig. 10. Mode of daily ground-tilting observed at Beppu Park.

The form of the daily ground-tilting variation is peculiar to the particular observation station, but its quality, not to mention its amplitude, is never constantly observed a day by day or season by season. An example is shown in Fig 10 in which is plotted the monthly averaged forms of daily ground-tilting observed at Beppu Park in 1937–1938 where the observation room is 3 m below the ground surface of alluvial sand. The complexity of the daily variation at one station is considered to have originated from the widely differing conditions

of solar radiation, level of underground water, and moisture content of soil.

On the relation between the underground depth of the observation room and the amplitude of daily and annual variation of ground-tilting observed, some discussions have been made by K. Sassa (**12**, **13**) and the writer. It is roughly concluded, from many tiltmetric observations at stations and rooms of widely differing conditions, that the daily and annual variations are seldom observed at a deep-seated observation room, that is to say, more than 20 m below the ground surface. In Table 2, some examples with regard to the relation between the amplitude of annual variation and room's depth are shown. But, concerning the preceding argument, exceptions are sometimes observed, namely, the comparatively large daily and annual variations observed at a deep seated room, and, on the contrary, the small daily and annual variations at a shallow seated room. These circumstances cannot definitely be confirmed unless a practical observation is carried out in the very room for the period of at least one year.

Table 2

| Station \ Condition | Underground depth of observation room | Mean double amplitude of annual variation of ground-tilting | Averaged value of secular ground-tilting per annum | Geological formation |
|---|---|---|---|---|
| Beppu 1 | 2 m | 16″ | 18″ | Alluvial sand |
| Beppu 2 | 2 | 22 | 13 | 〃 |
| Beppu 3 | 3 | 20 | 26 | 〃 |
| Beppu 4 | 5 | 2 | 7 | Volcanic layer |
| Kamigamo | 9 | 6 | 1 | Paleozoic |
| Yura | 30 | 0 | 22 | Mesozoic sandstone and shale |
| Kishu | 60 | 0 | 33 | Tertiary sandstone and shale |
| Hosokura | 160 | 0 | 17 | Tertiary |
| Makimine | 165 | 0 | 4 | Paleozoic |
| Ikuno 1 | 237 | 0 | 7 | Liparite |
| Ogoya | 300 | 0 | 82 | Tertiary tuff |
| Ikuno 2 | 326 | 0 | 27 | Liparite |
| Ikuno 3 | 719 | 0 | 22 | 〃 |
| Kamioka | 800 | 0 | 70 | Gneiss |

The small effect of barometric pressure change upon ground-tilting will be discussed elsewhere, though this effect seems to play an important role in the gravimetric observation.

The effect of rainfall upon ground-tilting is a most troublesome problem in cases of observation in a shallow seated room. The range of ground-tilting caused by heavy rainfall reaches several hundreds times as large as that of earth tidal change or several scores times as large as that of daily variation. The trouble exists not only

in large amplitude, but also in the complexity of behaviour strongly affected by its hysteresis, as is fully discussed by K. Sassa (**12**, **13**). Ground-tilting caused by heavy rainfall in a short duration of time shows a simple form, but it is sometimes difficult to treat fully the real manner of its recovery.

In Fig. 11 the amount of ground-tilting observed at Yura caused by rainfall in a comparatively short time is plotted against the amount of precipitation concerned. From this it should be simply stated that there is a linear relation, roughly speaking, between the amounts of ground-tilting and precipitation at Yura. And the precipitation less than 10 mm does not affect the ground-tilting in this case. The observation room

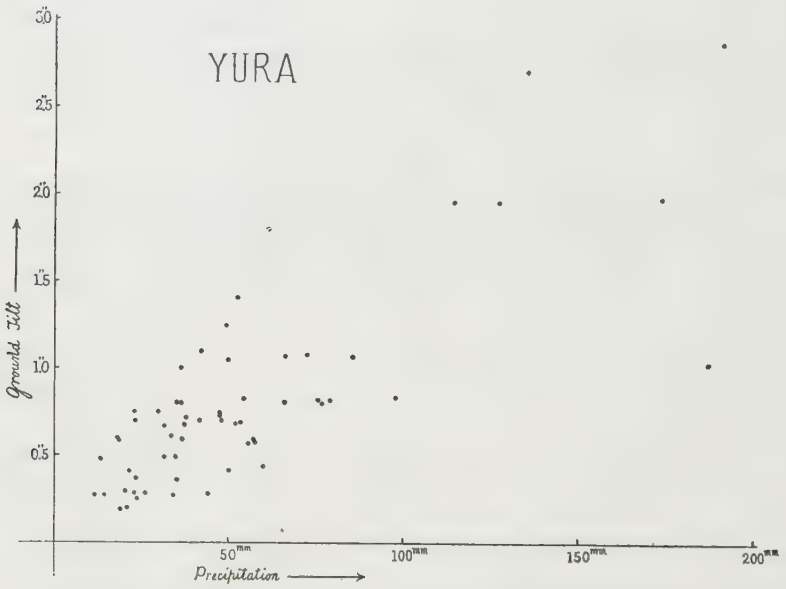


Fig. 11 Relation between the amount of ground-tilting caused by rainfall and the amount of precipitation observed at Yura.

is situated 30 m below the ground surface at the side of small mountain, the geological formation being tertiary sandstone and shale, and the ground sloping downward to the foot of the mountain by the effect of rainfall as though the mountain expanded by an increase of moisture content in the soil and rock, or the elasticity of soil and rock apparently decreased by rainfall.

In conclusion the disturbing meteorological effect should be reduced to as small an amount as possible for the purpose of studying the real, and, in ordinary cases, minute tilting motion of the ground such as those of earth tidal change or crustal deformation related to earthquake-occurrence, volcanic eruption, and other crustal change. One of the simple and effective ways to avoid the disturbance of meteorolo-

gical origin is to set up the observation room at appropriately deep underground in firm rock, say about 100 m～200 m below the ground surface. It is to be remarked here that the observation at a room too deep, that is to say, more than several hundred meters, is also inadequate for studying the secular ground-tilting, because the deep seated room is greatly deformed by tremendously great rock-pressure, thus disturbing the observation for real ground-tilting of the area concerned. Regarding this some detailed discussions will be made in the following section.

(*4*) *Local character in secular ground-tilting*

As seen in the foregoing figures, the individual characteristics of secular ground-

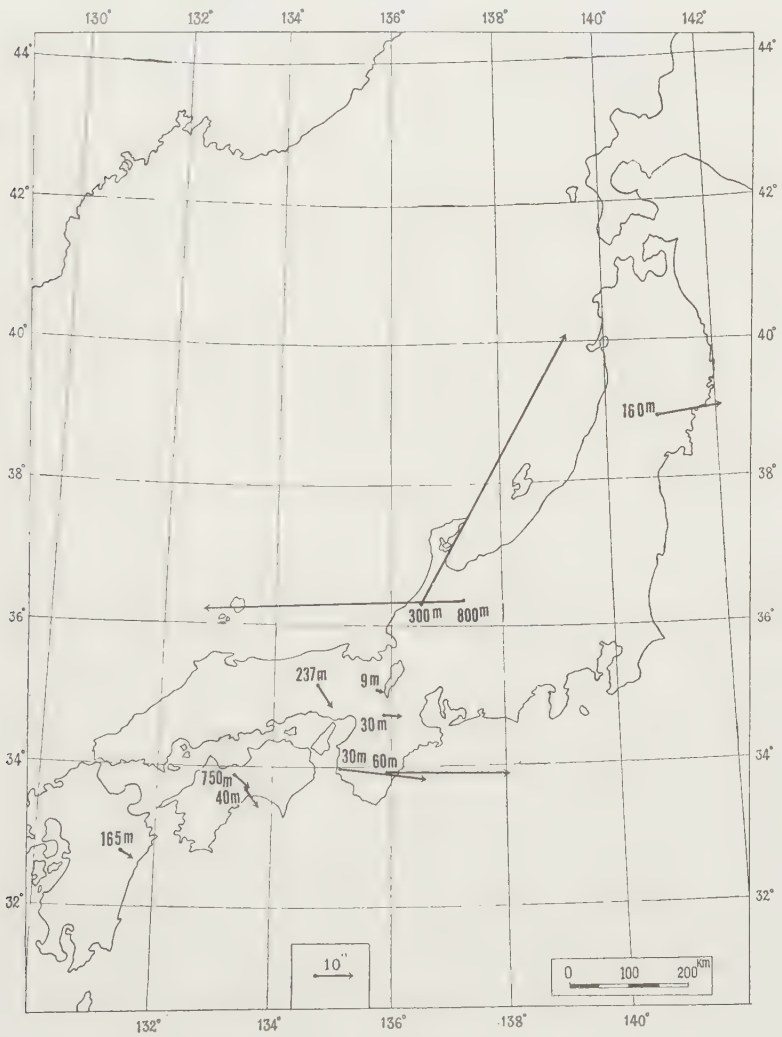


Fig. 12. Averaged amount and direction of secular ground-tilting per annum observed at some stations, the side-figure being the depth of observation room.

tilting observed at various stations are quite diversified displaying the peculiarity of their respective stations. These local characteristics are thought to originate from the local deformation of the ground related to the observation room conditions. The secular ground-tilting observed in a deep seated room is, in general, much greater in degree compared to the observation made in shallow seated room. This is simply interpreted to be conduced by the large deformation of the observation room in adit caused by a great rock-pressure constantly exerted consequently, secular ground-tilting being observed has naturally a large amplitude and strong peculiarity. As the secular ground-tilting observed in a shallow seated room is comparatively small without the influence of rock-pressure, it is considered to be suitable for the observation of secular ground-tilting, but it is inconvenient in the point of large disturbing influence by meteorological change as hitherto discussed. For this purpose a suitable observation room which is little affected by meteorological change and rock-pressure, should be selected for good observation. A close examination of these will be treated in the next section. In Fig. 12, some examples of the amount and direction of secular ground-tilting are shown. The arrow in the figure indicates the averaged amount and directions of downward tilting motion per annum, and the side figure indicates the depth of the observation room. Properly speaking, Fig. 13 is intended to show the diversity of secular ground-tilting and its local character, but it is both interesting and suggestive that a major part of tilt-vector tends toward the easterly direction with the exception of two stations. This may be an accidental coincidence, but it deserves a further investigation.

**5. Suitable observation station for secular ground-tilting**

For the purpose of investigating the earth-tidal tilting of the ground or the micro-tilting motion forerunning earthquakes and other minute ground-tilting, the tiltmeter must be maintained at a high sensitivity. The amplitude of the earth-tidal change is about 0″.03, and the forerunning micro-tilting as observed at Ikuno before the occurrence of the Tottori Earthquake in 1943 was 0″.09, and other change, generally called as micro-tilting motion of the ground is less than 0″.01. On the other hand, the ground-tilting caused by meteorological change reaches 1～10″, which greatly disturbs the observation of earth-tides and micro-tilting. As already mentioned, the meteorological effect is proportionately reduced by the use of a deep observation room, but conversely the effect by rock-pressure increases with depth.

In connection with the problems of observation room conditions the problem of relative merit of the type of tiltmeter should be simultaneously considered. I have already mentioned that a water-tube tiltmeter is considered to be better suited for the observation of secular ground-tilting than that of horizontal-pendulum type. But

the use of the water-tube tiltmeter is inconvenient for observing minute ground-tilting, such as earth-tides, phenomena forerunning earthquakes and other micro-changes, because of its low sensitivity and intermittent measuring ability. Then, for the purpose of observing all kinds of ground-tilting such as earth-tidal change, micro-tilting motion and secular ground-tilting at one station, the problems of what type of tiltmeter and at which depth the observation room is the most suitable, should fully be examined.

Concerning these problems of the ground-tilting's amplitude of annual variation, the average amount of secular variation per annum, and the observation-room depth, reference to Table 2 will reveal that three stations– i.e. Kamigamo, Makimine, and Ikuno (I)– are suitable stations. These three stations selected from about 33 stations functioning over a period of 20 years, are optimum selections because the daily and annual variation caused by meteorological and seasonal change, and, moreover, the most undersirable disturbances of rainfall are all negligible. The secular tilting-motion observed at these three stations is favourably small compared with those at other stations, this fact being the most reliable evidence of stable conditions of the observation room. There is no standard method for selecting the optimum observation room but it must be chosen to be suitable after one or two years' test observations at any given place. And it is eagerly hoped to set up both tiltmeter of horizontal-pendulum type and water-tube type at the same room of stable condition, and by this sort of simultaneous observation the nature of secular ground-tilting is expected to be rightly and fruitfully investigated.

### 6. Charcteristic tilting-motion connected with earthquake-occurrence

The large upheaval and subsidence of ground in the epicentral area before and after the occurrence of destructive earthquakes have been studied by the method of precise levelling and triangulation, and many detailed reports have been published in Japan. Especially these in case of the great Kwanto Earthquake in 1912 and the great Nankaido Earthquake in 1946 are representative in their amount of deformation. These results were all deduced from the data by re-survey of the epicentral area before and after the earthquake occurrence. On the other hand, the continuous observation of this kind of phenomena forerunning the destructive earthquake instead of intermittent surveys, have produced some reports recently published employing the continuous observation of tiltmeters and extensometers in the study of destructive earthquakes by K. Sassa and E. Nishimura (**21**) and others. K Sassa and E. Nishimura (**21**) have observed some minute but characteristic ground-tilting several hours before the occurrence of the destructive Tottori Earthquake in 1943, and several other earthquakes. I. Ozawa and I. Takada (**21**) have observed the forerunning phenomena taken from the results of the observation of ground-strain by extensometer in

case of Yoshino Earthquake in 1952 and others. The writer has also reported some examples of characteristic ground-tilting which were observed several months before the occurrence of destructive earthquakes in Daishoji in 1952, and Yoshino in 1952 (**14**, **15**, **16**, **21**).

In the present section, three cases of characteristic secular ground-tilting which are supposed to be connected with the occurrence of neighbouring destructive earthquakes are selected from our tiltmetric observations and discussed, especially, in point of reliability, taking the various disturbing effects mentioned above into consideration. The three cases concerned are the secular ground-tilting ones observed at Kamigamo, Ogoya and Yura. A discussion of these examples will follow:

(a) The Kamigamo investigation:

As already described, the tiltmetric observation at the Kamigamo Geophysical Observatory has been continued for 20 years, and its secular ground-tilting observed is exceedingly small and little disturbed by the meteorological effect, that is, the station is reasonably stable and suitable for observation of ground-tilting for a long period. During the period of observation any destructive earthquake within a 100 km radius from Kamigamo, with the exception of the Yoshino Earthquake, have not occurred, yet seven destructive earthquakes were felt within 200 km distance from Kamigamo. Their names, dates of occurrence, magnitude in Pasadena Scale, and distance of epicenter from Kamigamo are respectively listed as follows:

| Name | Date | Magnitude | Epicentral distance |
|---|---|---|---|
| Tottori | Sept. 10, 1943 | 7½ | 150 km |
| Tonankai | Dec. 7, 1944 | 8 | 150 |
| Mikawa | Jan. 13, 1945 | 7.1 | 120 |
| Nankaido | Dec. 21, 1946 | 8.2 | 230 |
| Fukui | June 28, 1948 | 7¼ | 130 |
| Daishoji-oki | Mar. 7, 1952 | 7¼ | 160 |
| Yoshino | July 18, 1952 | 7 | 70 |

In Fig. 7, the occurrence-time of these earthquakes is plotted in reference to the secular tilting curve. As may clearly be seen in the graph, characteristic ground-tilting had been observed for nearly one year before the occurrence of these destructive earthquakes with the exception of two cases at Mikawa and Daishoji-oki. At first sight we might question whether this strange character is to be interpreted as merely an accidental coincidence or really a significant fact. For further study this characteristic ground-tilting observed before the earthquake-occurrence is expressed in tilt-vector with the position of the epicenter of seven destructive earthquakes in Fig. 13. As clearly seen in the figure, these fine forerunning ground-tiltings are all pointing

to nearly the respective epicentral direction seen from Kamigamo, in other words, the ground commences a tilting motion downward to the direction of the epicenter nearly one year before the earthquake-occurrence. and continues its motion until the day of the earthquake, and after the earthquake, ceases or reverses its preceding motion. If this correspondence between the earthquake-occurrence and characteristic ground-tilting can be assumed to be real, this kind of tilt-metric observation should be considered to afford a promissing way to foretell the occurrence of destructive earthquake and reveal the nature of the earthquake itself.

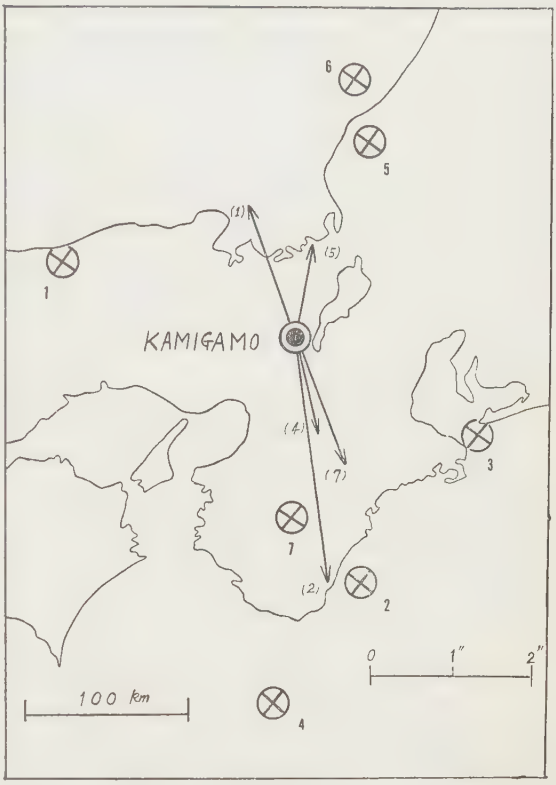


Fig. 13. Secular ground-tilting observed before the occurrence of destructive earthquakes observed at the Kamigamo Geophysical Observatory.

(1) Tottori, IX, 1943 (2) Tonankai, XII, 1944 (3) Mikawa, I, 1945 (4) Nankaido XII, 1946 (5) Fukui, VI, 1948 (6) Daishoji-oki, III, 1952 (7) Yoshino, VII, 1952.

(b) The Ogoya investigation:

Concerning the characteristic ground-tilting observed at Ogoya, some detailed papers have already been published (**14**). In this section a brief account will be given. A destructive earthquake named Daishoji-oki Earthquake occurred on March 7, 1952, 40 km NW of Ogoya. In this case, an abnormally large ground-tilting was observed, as shown in Fig. 8m, especially conspicuous in the B-component which records the ground-tilting in the EW-direction. It began during the first three months before the earthquake-occurrence, and the total amount and direction are estimated to be nearly 70″ in three months and in the same direction of NW when both A and B components are taken into account (see Fig. 4 in (**21**)). This severe tilting motion was reversed several days after the earthquake-occurrence, as seen in the B-component in Fig. 8m, but it recovered its original state after nearly one and half years. The amount of secular ground-tilting observed at Ogoya is, by nature, enormously large as seen in Fig. 8m and Table 2, according to the weak geological formation of tertiary tuff.

But, the to-and-fro tilting motion as observed in the B-component in the present case is supposed to be a real crustal deformation related to the earthquake, because the large, secular ground-tilting caused by the deformation of the adit-room affected by a powerful rock-pressure of 100 bars, is generally considered to be linearly increasing with time toward a certain direction. That the characteristic ground-tilting observed before the earthquake-occurrence at Ogoya shows also the downward motion to the direction of the epicenter seen from Ogoya, is in good accord with those discussed in the Kamigamo case, and increases the reliability of the existence of the phenomena of ground-tilting foretelling the earthquake-occurrence.

(c) Tne Yura investigation:

The observation at Yura is greatly disturbed by the effect of rainfall, and its secular variation is also considerably large as described in Table 2. But, as the annual variation is little observed, and moreover, the prominent earthquakes have frequently occurred in the neighbourhood of Yura, the relation between the secular ground-tilting and occurrence of earthquake is conveniently discussed in spite of rather poor

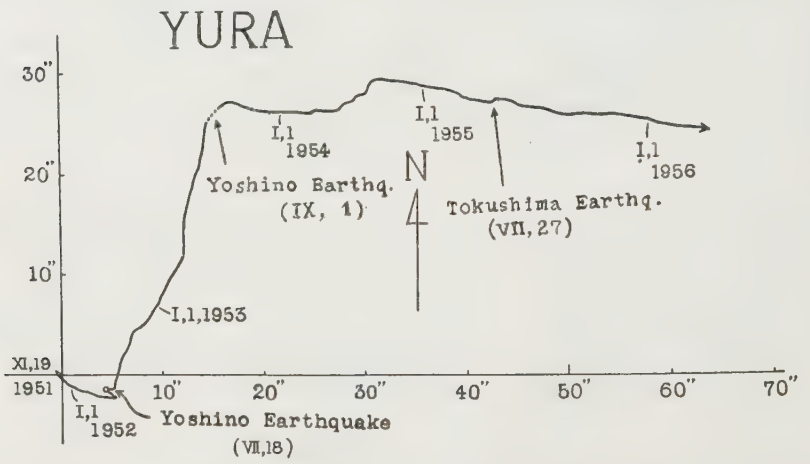


Fig. 14. Vector-representation of secular ground-tilting observed at Yura Observation Station.

Arrow indicates the occurrence time of large earthquakes in the neighbourhood of Yura.

conditions of the observation room. The secular ground-tilting observed in two components and the composed tilt-vector are shown in both Fig. 8h, and Fig. 14. During the observation period, three destructive earthquakes occurred in the neighborhood of Yura. Namely, the epicenter of the Yoshino Earthquake, July 18, 1952, was 60 km distant and in an E-direction from Yura; the earthquake in Yoshino district, September 1, 1953, had nearly the same epicenter as that in 1952; and the epicenter of the earth-

quake near Tokushima, July 27, 1955, was nearly 60km distant and in W-direction from Yura. Their seismic magnitudes are all nearly 7 using the Pasadena Scale as reference. In the case at Yura, only the secular ground-tilting observed before the occurrence of the Yoshino Earthquake showed a like tendency such as those discussed in the preceding two cases of Kamigamo and Ogoya. Namely, the ground has tilted downwards to the direction of epicenter (E-direction) more thau a half year before the occurrence, and after that the direction of ground-tilting has changed in a nearly orthogonal direction (NNE). With regard to the other two earthquakes, this relation does not hold. But it is to be remarked that the time of occurrence in other two earthquakes are both situated at the turning point on the curve of tilt-vector. Especially the earthquake in Yoshino district in 1953 affords a conspicuous example of this relation. Further investigation is eagerly desirable to advance the knowledge in this research field.

In concluding this section, it is strongly suggested that characteristic secular ground-tiltings ever observed at some stations, in nearly a period from several months to one year before the occurrence of destructive earthquakes, are supposed to be the really existing phenomena intimately connected to the earthquake. It will afford, in the near future, a powerful clue to foretell the occurrence of destructive earthquakes and advance knowledge on the nature of earthquakes.

**Acknowledgments**

The writer wishes to express his cordial thanks to Prof. E. Nishimura for his kind guidance throughout this study and also to Prof. K. Sassa for his valuable advice. It is a great pleasure for the writer to record with thanks the sympathy and the kind assistance given by the observers in many observation stations concerned in this study. The expenses for the observation were defrayed partly by a Grant in Aid for Scientific Research from the Ministry of Education, and partly by the Research Fund of the Disaster Prevention Research Institute.

REFERENCES

1. C. Tsuboi, Note on the deformation of the Earth's crust as determined by precise geodetic means, Japanese J. Astron. and Geophys., **10** (1933), 93.
2. N. Miyabe, A summary of the results of studies made in Japan during the period 1933–1938 on deformation of the Earth's crust, Proc. of the Sixth Pacific Congress, (1938), 151.
3. N. Miyabe, Vertical earth movement in Nankai district, Bull. Geograph. Survey Inst., **4** (1955), 1.
4. M. Ishimoto, Silica tiltmeter of horizontal pendulum type (in Japanese), Zisin, **1** (1929), 17.
5. M. Ishimoto, Construction d'un pendule horizontal de quartz et observations sur les variations de l'inclination de la surface terrestre, Japanese J. Astron. and Geophys., **6** (1928), No. 2.

6. U. INOUE and T. SUGIYAMA, Report on observation of ground-tilting observed at Mt. Tsukuba (in Japanese), Bull. Eartq. Res. Inst., Tokyo Univ., **3** (1930), 346.
7. K. SASSA and E. NISHIMURA, On phenomena forerunning earthquakes, Trans. Amer. Gephys. Union, **32** (1951), 1.
8. T. HAGIWARA, Observation of changes in the inclination of the Earth's surface at Mt. Tsukuba (I), Bull. Earthq. Res. Inst., Tokyo Univ., **16** (1938), 366; (II), ditto, **19** (1941), 218; (III), ditto, **25** (1947), 27.
9. H. ARAKAWA, Ground-deformation caused by daily and annual variations of ground-temperature. (in Japanese), Meteorolog. Mag., Ser. 2, **10** (1932), 637.
10. J. KAWASE, Observation of ground-tilting at Momoyama. (in Japanese), Zisin **5** (1933), 52.
11. T. KOGURE, T. KIMURA and T. MATSUDA, Observation of ground-temperature and ground-tilting. (in Japanese), Zisin **6** (1934), 640.
12. K. SASSA, Ground deformation caused by meteorological changes. (in Japanese), Japanese J. Astron. and Geophys., (in Japanese), **1** (1940), 17.
13. K. SASSA, Ground deformation affected by meteorological variation. (in Japanese), Report by Hattori Hôkô Kai, No. 10 (1943), 158.
14. K. HOSOYAMA, Characteristic tilt of the ground that preceded the occurrence of the strong earthquake of Mar. 7, 1952, Journ. Phys. of the Earth, **1** (1952), 75.
15. E. NISHIMURA and K. HOSOYAMA, On tilting motion of the ground observed before and after the occurrence of an earthquake, Trans. Amer. Geophys. Union, **34** (1953), 597.
16. K. HOSOYAMA,On a mercury tiltmeter and its application, Bull. Disaster Prevention Res. Inst., Kyoto Univ., No. **6** (1953), 17.
17. E. NISHIMURA, On earth tides, Trans. Amer. Geophys. Union, **31** (1950), 357.
18. A. IMAMURA, Chronic earth-tilting in the Kii-Peninsula: An indication of the accumulation of seismogenic forces, Proc. Imp. Acad., **5** (1929), No. 4.
19. A. IMAMURA, A comparison of crustal deformation between Kii-Peninsula and Muroto-Peninsula, (in Japanese), Zisin **6** (1934), 535; **9** (1937), 200; **11** (1940), 213.
20. A. IMAMURA, On crustal deformation preceding earthquakes, Japanese J. Astron. and Geophys., **10** (1932), 81.
21. K. SASSA, and E. NISHIMURA, On phenomena forerunning earthquakes, Publ. Bur. Central Seism. Intern., Sér. A, Trav. Scientif., Fascicule 19, 1956.

## CONTENTS

**Diffraction of Electromagnetic Waves by a Circular Cylinder of Infinite Length**

By *Isao Takahashi, Tadashi Watanabe and Kiichi Tanimoto* ..... 209

**Transient Phenomena in the Wave Guide**

By *I. Takahashi and T. Watanabe* ..... 221

**On Some Relation between Atmospheric Ions and Natural Radioactivity**

By *Sigeru Okabe* ..... 231

**On the Observation of Secular Phenomena of the Tilting Motion of the Ground**

By *Kennosuke Hosoyama* ..... 253

*Printed by NIPPON INSATSU SHUPPAN*

*Fukushima, Osaka*